Mele *et al. Cardiovascular Ultrasound* (2025) 23:13
https://doi.org/10.1186/s12947-025-00347-1

Cardiovascular Ultrasound

REVIEW Open Access

Left ventricular flow dynamics by cardiac imaging techniques in heart failure patients: state of the art

Donato Mele[1,2*], Lorenzo Serio[1], Riccardo Beccari[1], Antonella Cecchetto[1], Stefano Nistri[1,3] and Gianni Pedrizzetti[4]

Abstract

Background The evaluation of left ventricular (LV) flow dynamics is a novel approach to assessing LV function that goes beyond traditional metrics. This approach has been applied to patients with heart failure (HF), providing valuable insights that are discussed in this review, with the aim of enhancing our understanding of LV function in the context of the HF syndrome.

Methods The analysis of LV flow dynamics is typically conducted using ultrasound and magnetic resonance imaging (MRI) techniques, primarily including particle image velocimetry echocardiography, Vector Flow Imaging, HyperDoppler, and four-dimensional flow MRI. A variety of parameters can be obtained that describe the geometry of the LV vortex, vorticity, kinetic energy, energy dispersion, as well as the amplitude and direction of the hemodynamic forces within the LV cavity.

Results In normal subjects, vortex formation plays a crucial role in optimizing LV filling, diastolic-systolic coupling, and energy transfer during systolic ejection. In patients with HF, alterations in vortex structure and dynamics have been associated with both systolic and diastolic LV dysfunction, demonstrating the potential to diagnose early LV dysfunction. Furthermore, these alterations have been linked to LV remodeling and thrombus formation. Several studies have also explored intracardiac flow metrics as biomarkers for guiding HF treatments, including pharmacological interventions, cardiac resynchronization therapy, and LV assist devices.

Conclusions Currently available data suggest that the evaluation of LV flow dynamics can have diagnostic and prognostic utility in HF. However, large-scale, multicenter, and prospective studies are needed, particularly to validate therapeutic implications.

Keywords Heart failure, Intracardiac flow dynamics, Cardiac vortex, Hemodynamic forces

*Correspondence:
Donato Mele
donato.mele@unipd.it
[1]Department of Cardiac Thoracic Vascular Sciences and Public Health, University of Padova, Via Giustiniani, 2, 35128 Padova, Italy
[2]Cardiac Unit, Ravenna33 Clinic, Via Bini, 1, 48124 Ravenna, Italy
[3]Cardiology Service, CMSR Veneto Medica, Via Vicenza 204, 36077 Altavilla Vicentina (VI), Italy
[4]Department of Engineering and Architecture, University of Trieste, Trieste, Italy

© The Author(s) 2025. **Open Access** This article is licensed under a Creative Commons Attribution-NonCommercial-NoDerivatives 4.0 International License, which permits any non-commercial use, sharing, distribution and reproduction in any medium or format, as long as you give appropriate credit to the original author(s) and the source, provide a link to the Creative Commons licence, and indicate if you modified the licensed material. You do not have permission under this licence to share adapted material derived from this article or parts of it. The images or other third party material in this article are included in the article's Creative Commons licence, unless indicated otherwise in a credit line to the material. If material is not included in the article's Creative Commons licence and your intended use is not permitted by statutory regulation or exceeds the permitted use, you will need to obtain permission directly from the copyright holder. To view a copy of this licence, visit http://creativecommons.org/licenses/by-nc-nd/4.0/.

Background

Heart failure (HF) is a clinical syndrome caused by structural and/or functional cardiac abnormalities that result in reduced cardiac output and/or elevated intracardiac pressures at rest or during stress [1]. Patients with HF typically exhibit myocardial, valvular, and electrical dysfunction, often leading to enlarged cardiac chambers.

Traditional assessments of cardiac function focus on well-established parameters obtained through cardiac imaging techniques, such as left ventricular ejection fraction (LV-EF), which allows for the distinction between HF with reduced and preserved LV-EF (HFrEF and HFpEF, respectively), as well as the estimation of LV filling pressures [2]. However, discrepancies may exist between patients' symptoms and these imaging parameters, and patients with varying degrees of compensation may present with similar echocardiographic indicators of cardiac dysfunction. Thus, there is still a significant need for appropriate imaging assessments that go beyond conventional parameters in HF patients.

Intracardiac flow analysis aids in visualizing and quantifying flow dynamics throughout the cardiac cycle [3]. This analysis has proven to be particularly promising in several cardiac diseases, especially in the context of valvular heart diseases [3, 4]. In this review, we aim to describe the clinical applications of LV flow dynamics in the study of HF patients, with the objective of enhancing the understanding of cardiac function and hemodynamics in these individuals, as well as evaluating whether this approach can improve the early detection of cardiac dysfunction and assist in predicting cardiovascular outcomes.

Imaging techniques to evaluate LV flow dynamics

Different cardiac imaging techniques can be used to assess LV flow dynamics (Fig. 1). The echocardiographic technique initially applied is based on an adaptation of Particle Image Velocimetry (PIV) and is commonly referred to as echo-PIV [3]. The echo-PIV technique relies on the intravenous injection of a low dose of ultrasound contrast agents, specifically microbubbles that exhibit rheological behavior similar to that of red blood cells, thus acting as tracers for blood flow. The echo-PIV technique has been validated and used in several clinical studies. The best results are obtained when the quality of the ultrasound image is high, the frame rate is elevated,

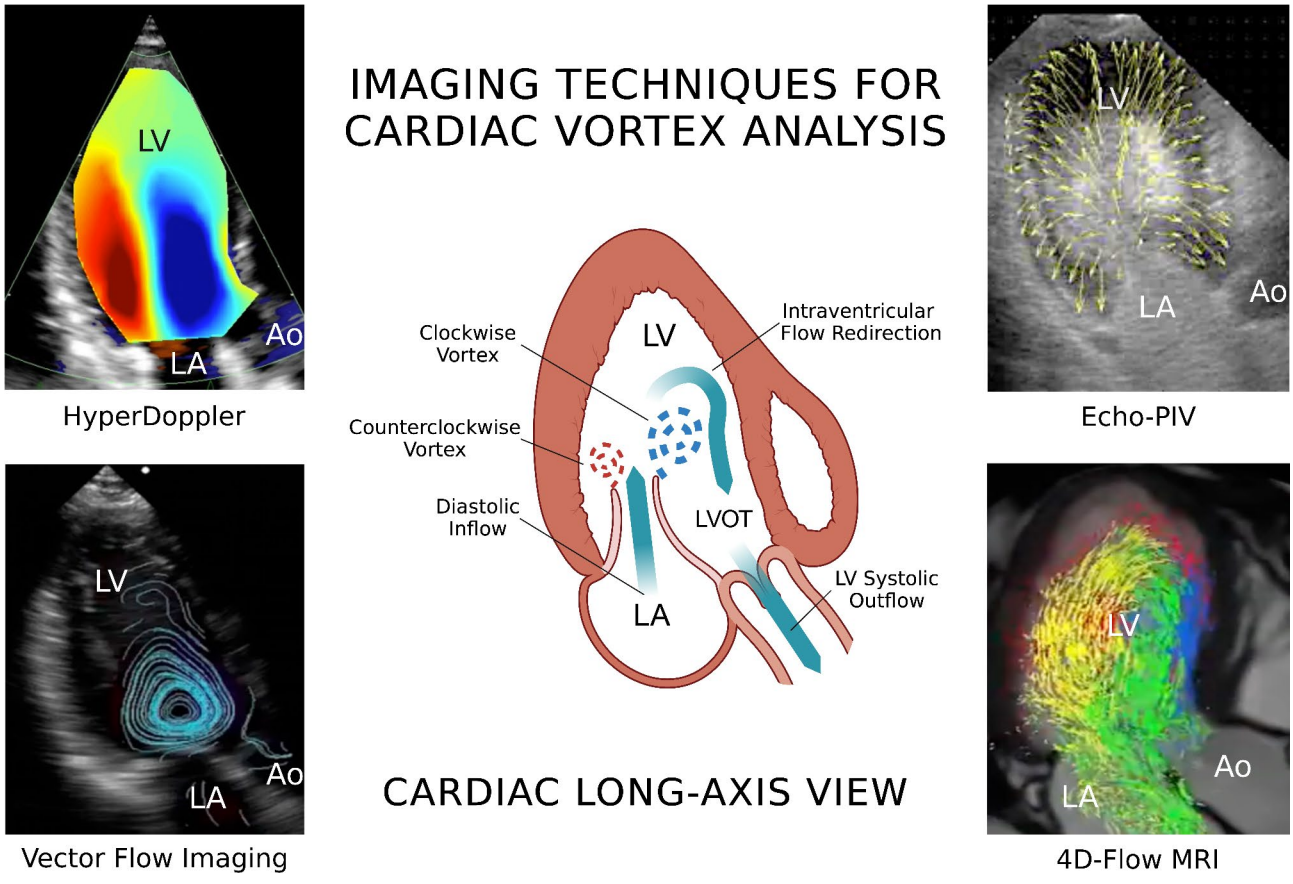

Fig. 1 Schematic of a long-axis view of the heart (middle) illustrating vortex motion inside the left ventricle (LV) cavity. On both the right and left side, image examples of four different cardiac imaging techniques for assessment of intracardiac flow dynamics are shown. Ao: aorta. Echo-PIV: echocardiographic particle imaging velocimetry. 4D-Flow MRI: four-dimensional flow magnetic resonance imaging. LA: left atrium. LVOT: left ventricle outflow tract

and the microbubbles are evenly distributed within the LV cavity.

In recent years, other echocardiographic techniques have been developed that allow for the assessment of intracardiac blood flows without the use of contrast agents. Some techniques are based on color Doppler echocardiography, while others rely on blood speckle tracking. Color Doppler-based techniques include Vector Flow Mapping (VFM, Hitachi, Japan) [3] and HyperDoppler (Esaote, Genoa, Italy) [5]. Blood speckle tracking forms the basis of Blood Speckle Imaging (BSI, GE, Milwaukee, USA), which enables direct assessment of blood velocity vectors without the mathematical assumptions inherent in color Doppler-based approaches [3]. This technique, however, is currently applicable only to high-frequency transesophageal and pediatric probes. Regardless of the ultrasound technique used, the evaluation of intracardiac flows is typically performed in the echocardiographic apical long-axis view, which allows for the visualization of both inflow and outflow from the LV in the same image.

Magnetic resonance imaging (MRI) enables three-dimensional volume acquisition with velocity parameters encoded in three spatial directions using four-dimensional (4D) time-resolved phase-contrast imaging, commonly referred to as 4D-flow MRI [3]. Cardiac computed tomography (CCT) does not inherently measure flow quantities such as blood velocity or pressure. However, recent advances have integrated it with computational fluid dynamics (CFD), resulting in 4D-flow CCT [6]. CFD is not limited to CCT; it is also available in MRI and echocardiography [7, 8], expanding the repertoire of cardiac imaging techniques available for evaluating intracardiac flow dynamics.

Physiology of LV flow dynamics

Normally, when blood flow enters the LV, it gives rise to the formation of a compact, ring-shaped vortex structure that surrounds the mitral valve leaflets and is located distally to the leaflets themselves within the LV cavity [3]. In a long-axis view of the LV, the vortex ring appears as a pair of counter-rotating vortices: one situated distally to the anterior leaflet of the mitral valve, which is larger and rotates clockwise, and one located distally to the posterior leaflet, which is smaller and characterized by counterclockwise rotation (Fig. 1). The formation of the vortex, as described, results from an optimal interaction between the geometry of the LV chamber, the morphology of the mitral valve apparatus, and the normal electrical conduction system, which facilitates the harmonious contraction of the LV walls. In particular, the physiological eccentric position of the mitral valve orifice and the asymmetry of its leaflets are the main determinants of the vortex's asymmetry.

Throughout the cardiac cycle, variations in the vortical flow have significant physiological implications [3] (Fig. 2). The variations that occur in the early part of diastole promote ventricular suction and thus facilitate the filling of the LV, while subsequent variations favor the coupling between diastole and systole, ultimately aiding the ejection of blood from the LV. More precisely, the vortex generated during the rapid filling of the LV prevents the divergence of incoming blood, reducing collisions with the LV walls and minimizing the dissipation of kinetic energy (KE). During diastasis, the vortex stores KE in its rotational movement. Subsequently, during isovolumetric contraction time (IVCT), flow is redirected from the apex toward the LV outflow tract (LVOT), merging with a wake vortex in the subvalvular region. This assists in the closure of the mitral valve, and since flow acceleration does not cease with mitral valve closure but rather continues during the IVCT, it also preserves KE, making the flow immediately available for ejection.

In summary, the vortical structure ensures both regular LV filling and a smooth transition toward ejection, thereby achieving optimal diastolic-systolic coupling [3].

Measures of LV flow dynamics

Blood flow dynamics within the LV cavity can be assessed both visually and quantitatively using several parameters [3, 9] (Table 1).

Geometric measures include vortex area, length, width, and depth (or position). These parameters can be expressed in metric units or as dimensionless indices when normalized to the size (area, length, and width) of the entire LV chamber.

Vorticity measures encompass vortex circulation and strength or intensity. These parameters can be either positive or negative, depending on the direction of blood flow: negative for clockwise flow and positive for counterclockwise flow.

The development of vortex rings is most often quantified using vortex formation time (VFT), a dimensionless parameter [10]. The optimal VFT ranges from 3.3 to 5.5 in healthy subjects.

Energetic properties include kinetic energy (KE), kinetic energy loss (KEL) or dissipation (KED), and kinetic energy fluctuation (KEF). Energy measures can vary with age [11].

Intracardiac hemodynamic forces (HDFs) reflect intraventricular pressure gradients (IVPGs), specifically their intensity during different phases of the cardiac cycle or their deviation from the axial direction [12, 13] (Fig. 3).

Finally, various types of shear stress (such as wall shear stress, viscous shear stress, and Reynolds shear stress) can be calculated.

Measures of intracardiac flow dynamics can be expressed as mean values throughout the cardiac cycle

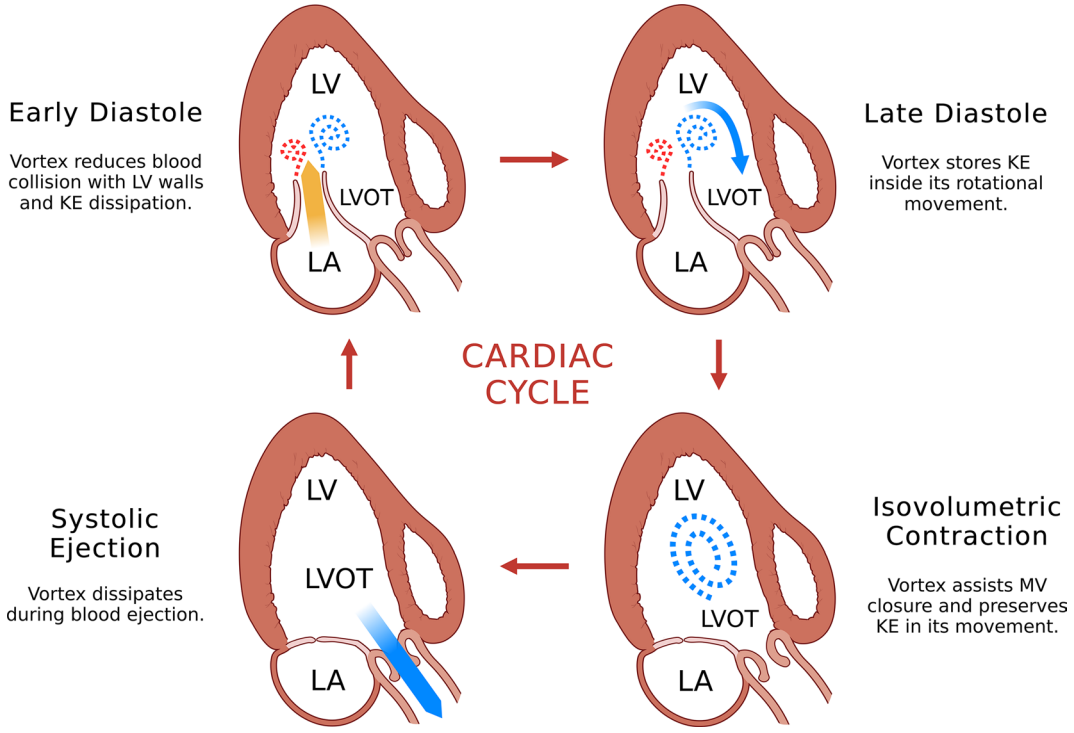

Fig. 2 Normal flow pattern inside the left ventricular (LV) cavity during a cardiac cycle in a schematic drawing of the long-axis view of the heart. KE: kinetic energy. LA: left atrium. LVOT: left ventricle outflow tract. MV: mitral valve

or evaluated during specific phases of the cycle (for instance, during LV early filling, late filling, or systole). Additionally, measures of vortex properties can be expressed using specific units or as dimensionless ratios (for example, indexing the value of a vortex property to the value in the entire cardiac chamber). This applies to geometric measures, as mentioned above, as well as to vorticity measures.

In one study [14], the main vortex core measurements obtained using a color Doppler-based technique correlated reasonably well with phase contrast-MRI measurements. However, other authors have reported that the agreement between different modalities studying intraventricular flow is low [15], although the level of agreement depends on the parameters used in the comparison and their inherent variability. In this review, results obtained from ultrasound and MRI-based techniques will generally be presented separately.

Functional components of LV end-diastolic volume

First described by Bolger et al. [16] and later by Eriksson et al. [17] using 4D-flow MRI, the LV end-diastolic volume (EDV) can be divided into four functional flow components: direct flow (DF), retained inflow, delayed ejection flow, and residual volume (Fig. 4).

The DF refers to the blood that enters the LV during diastole and exits the LV during the subsequent systole. Retained inflow is the blood that enters the LV during diastole but does not leave during the next systole. Delayed ejection flow consists of blood that begins and remains in the LV during diastole and exits during systole in the following beat. The residual volume is the blood that remains within the LV for at least two cardiac cycles. Together, the retained inflow and the residual volume constitute the non-ejecting portion of the LV EDV.

In a normal subject, the DF component, which represents the subset of LV inflow that is directly available for ejection, is the largest part of the LV EDV (Fig. 4) and exhibits more favorable characteristics for subsequent ejection compared to the other flow components. Specifically, at the time of IVCT, the DF has the highest KE, the shortest distance to the LVOT, a smaller angle of motion relative to the LVOT, and greater linear momentum directed towards the LVOT compared to the non-ejecting components. In other words, since the predominant trajectory of the DF in pre-systole is towards the LVOT, the preserved KE of this flow component may indicate that less work is required for the ejection of stroke volume (SV).

The retained inflow and the residual volume do not exit the LV during the subsequent systole, thus their KE does not directly contribute to ejection. However, their KE distribution and velocity may facilitate ejection by creating an efficient pathway for the SV during diastole.

Table 1 Main properties of intracardiac vortex, energy and hemodynamic forces

Property	Description and explanation	Calculation
Vortex area (VA, cm^2) and VA index (VAi, dimensionless)	It can be measured at specific point in time or throughout the cardiac cycle (total vortex area). The VAi is the ratio between the total vortex area and the LV area.	VAi = total VA/LV area.
Vortex length index (VLi, dimensionless)	It can be measured at specific point in time or throughout the cardiac cycle (total vortex length). The VLi is the ratio between the total vortex length and the LV length.	VLi = total vortex length/LV length.
Vortex depth index (VDi, dimensionless)	It is the vertical position of the center of the vortex (the distance of its center from the mitral annular plane) relative to the LV long-axis.	VDi = distance of vortex center from LV base/LV long-axis
Vortex circulation (cm^2/s). If normalized with the LV total vorticity, it is dimensionless.	It is the integral of the vorticity inside the vortex. It may refer to the clockwise (CW) or counterclockwise (CCW) vortex.	Circulation = vortex vorticity/LV total vorticity.
Vortex strength (VS) or intensity (VI, cm^2/s)	It is the total amount of vortex vorticity. It refers to the sum of the CW and CCW vortex circulation.	VS = CW circulation + CCW circulation.
Vortex formation time (VFT, dimensionless)	It is a measure of fluid propagation efficiency through the LV and therefore an indicator of overall cardiac health. It quantifies the process of vortex ring formation in the LV.	$VFT = 4 \times (1 - \beta) / \pi \times \alpha^3 \times$ LV-EF
Kinetic energy (KE, mJ) and KE index (KEi, mJ/ml)	It is the KE contained in the LV cavity area (in two-dimensional images) or volume (in three-dimensional images). It can be normalized with the LV area/volume, to give average KE and remove dependence from the LV size. The KE of the intraventricular flow depends on blood flow velocity and density.	KE = integral over the LV cavity of $1/2\rho\ (vx^2 + vy^2 + vz^2)$, where vz is present only in three-dimensional analysis; ρ is the blood density ($\rho = 1050\ Kg/m^3$).
Viscous KE dissipation (kED) or loss (kEL, mW/m or J/m·s) or kED index (kEDi, dimensionless).	It is the amount of KE, ΔKE, dissipated into the heart (by viscous friction) during the cardiac cycle. The total KE dissipation is the value integrated over the entire LV; it can be normalized with the average KE (kEDi) to avoid direct dependence from the LV size.	kEDi = integral over the LV cavity and over the heartbeat of the rate of KE dissipation (double scalar product of deformation and stress tensors).
Flow force angle φ or flow momentum angle (degrees)	Quantitative parameter describing the orientation of the LV hemodynamic forces, that is, the dominant direction of flow momentum identified by an average angle, that lies between 0° (corresponding to longitudinal forces) and 90° (when forces are transverse). Longitudinally oriented hemodynamic forces (directed along the "base-to-apex" axis) dominate in the normal LV during both systole and diastole, concordant with the predominant directions of acceleration/ deceleration of the LV inflow through the mitral valve and outflow through the aortic valve. In a pathologically asynchronous condition, the hemodynamic forces develop transverse components (generally from the infero-posterior to the antero-septal wall of the LV) and the flow force angle increases.	The angle φ is obtained by $\sin^2\varphi$ by the integral during the heartbeat of F x $\sin^2\theta$, normalized by the integral of F, where F(t) and θ(t) are the magnitude and orientation respect to the LV axis, of the force at every instant during the heartbeat.

CW: clockwise. CCW: counterclockwise. KE: kinetic energy. KEi: kinetic energy index. kED: kinetic energy dissipation. kEDi: kinetic energy dissipation index. kEL: kinetic energy loss. LV: left ventricle. MRI: magnetic resonance imaging. VA: vortex area. VAi: vortex area index. VDi: vortex depth index. VI: vortex intensity. VLi: vortex length index. VS: vortex strength

While 4D-flow MRI is the reference technique for analyzing blood transport in the LV, similar information has also been obtained using ultrasound [18–20].

LV flow dynamics alterations as a cause of LV remodeling

Alterations in LV flow dynamics independently modulate regional wall stress distribution. Stable vortex patterns support efficient LV filling and ejection by ensuring even distribution of pressure and wall stress, as mentioned previously. When physiological vortex dynamics is disrupted, abnormal transverse intraventricular pressure gradients (IVPGs) and turbulence emerge. These disturbances consequently lead to focal regions of heightened wall stress, which are the result of localized mechanical forces imbalances [21] (Fig. 5).

Abnormal flow patterns produce regions of transient, unpredictable stress spikes along the LV wall. This is in contrast to a uniform elevation of endoventricular pressure, where wall stress increases homogeneously. Instead, the irregular flow, with its associated turbulent shear forces and dynamic pressure gradients, can create "hot spots" of mechanical stress able to trigger mechano-responsive pathways, which translate mechanical stimuli into intracellular signals [22] (Fig. 6).

There are several mechanisms for translating mechanical stimuli. Integrins, which anchor the extracellular matrix to the cytoskeleton, respond to changes in wall stress by activating downstream pathways, such as focal adhesion kinase and mitogen-activated protein kinases, promoting hypertrophic gene expression and extracellular matrix remodeling [23, 24]. Transient receptor potential channels facilitate calcium influx under shear stress, triggering calcineurin-mediated activation of nuclear factor of activated T-cells, a key regulator of hypertrophic and fibrotic responses [25]. Similarly, Piezo1, a mechanically gated ion channel, contributes to calcium-dependent signaling and inflammatory cascades

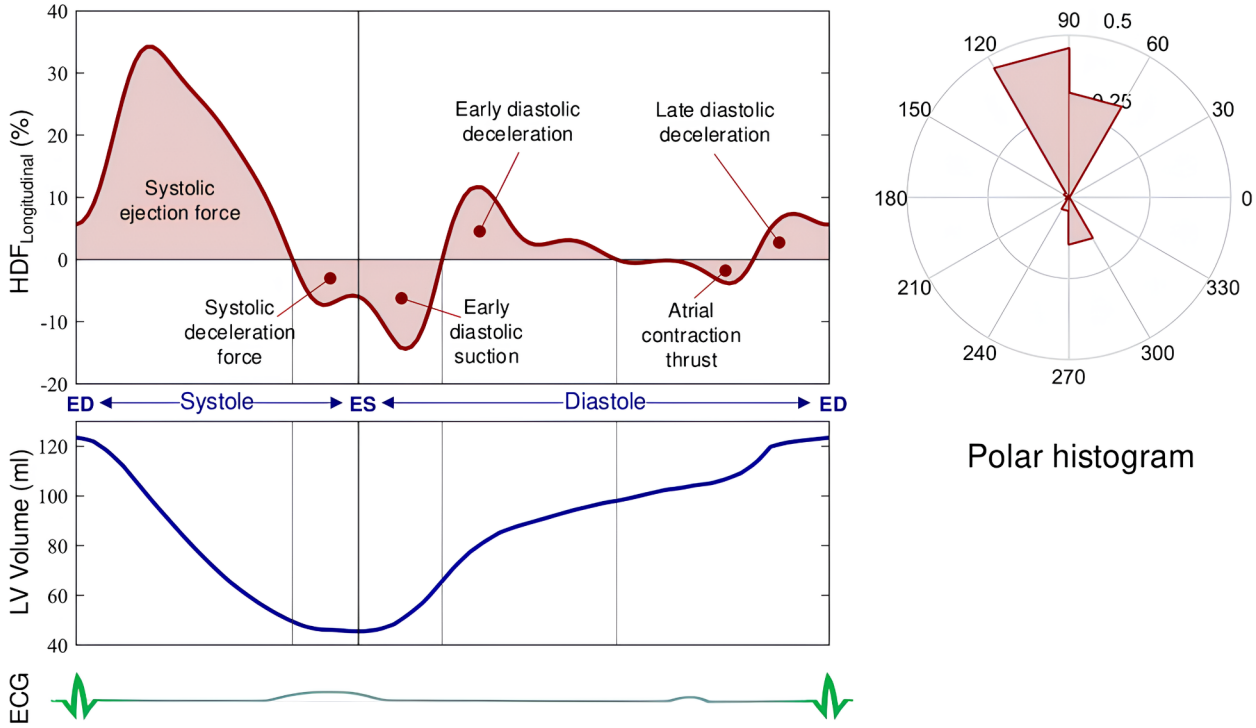

Fig. 3 Left ventricle (LV) longitudinal (apical-basal) hemodynamic forces (HDFs) in a normal athlete. *Left top*. Time profile of the apical-basal LV HDFs. The main intracardiac events during individual time intervals are indicated, together with markers of end-diastole (ED) and end-systole (ES). *Left bottom*. LV volume curve. *Right*. Intensity-weighted polar histogram, showing the distribution and intensity of the LV HDFs during the entire heartbeat as red isosceles triangles. HDFs are directed longitudinally (apex-base direction). ECG: electrocardiogram

in response to abnormal flow patterns [26]. These mechano-transductive processes are further modulated by titin, a sarcomere-spanning protein that plays a critical role in sensing and responding to mechanical stress. Titin not only regulates sarcomeric tension but also acts as a mechanosensitive hub, linking sarcomeric dynamics to the transcriptional regulation of stress-responsive and hypertrophic genes [27].

While these pathways may initially serve a compensatory role, their prolonged activation in response to chronic flow abnormalities and localized stress fluctuations can lead to pathological hypertrophy, fibrosis, and extracellular matrix remodeling, ultimately driving LV decompensation.

The reactivation of fetal gene programs under chronic mechanical stress is another hallmark of maladaptive myocardial remodeling. This phenomenon underscores the pivotal role of mechanical signals in regulating cardiac structure and function. During embryonic development, vortical forces from intracardiac blood flow act as critical regulators of gene expression, triggering the biochemical pathways involved in morphological cardiovascular development [28, 29]. This developmental paradigm is mirrored in pathological states, where mechanical stress from aberrant blood flow and ventricular stretch reactivates "fetal memory" genetic programs [21].

This reactivation process involves the upregulation of brain natriuretic peptide and atrial natriuretic peptide, biomarkers of myocardial stress, along with the re-expression of embryonic isoforms of contractile proteins, such as β-myosin heavy chain and skeletal α-actin [30]. These shifts in gene expression contribute to a less efficient and more energetically demanding myocardial phenotype, which is a key characteristic of the failing heart.

Alterations in LV flow dynamics for HF diagnosis

Analyzing LV flow dynamics can serve as a tool in diagnosing HF by identifying LV systolic and diastolic dysfunction, detecting early LV dysfunction, and assessing the risk of LV thrombosis, particularly in patients with ischemic cardiomyopathy (ICM).

Systolic dysfunction. LV systolic dysfunction is determined not only by loss of contraction force of the LV myocardium but is also influenced by altered diastolic-systolic coupling, which results from the reduced transmission of early diastolic KE to end-diastole. Therefore, the evaluation of DF and KE is critical in HF patients, especially at end-diastole.

Echocardiographic studies. The results of key echocardiographic studies are summarized in Table 2.

Hong et al. [31] observed that, in patients with reduced LV-EF, vortex morphology was consistently shorter,

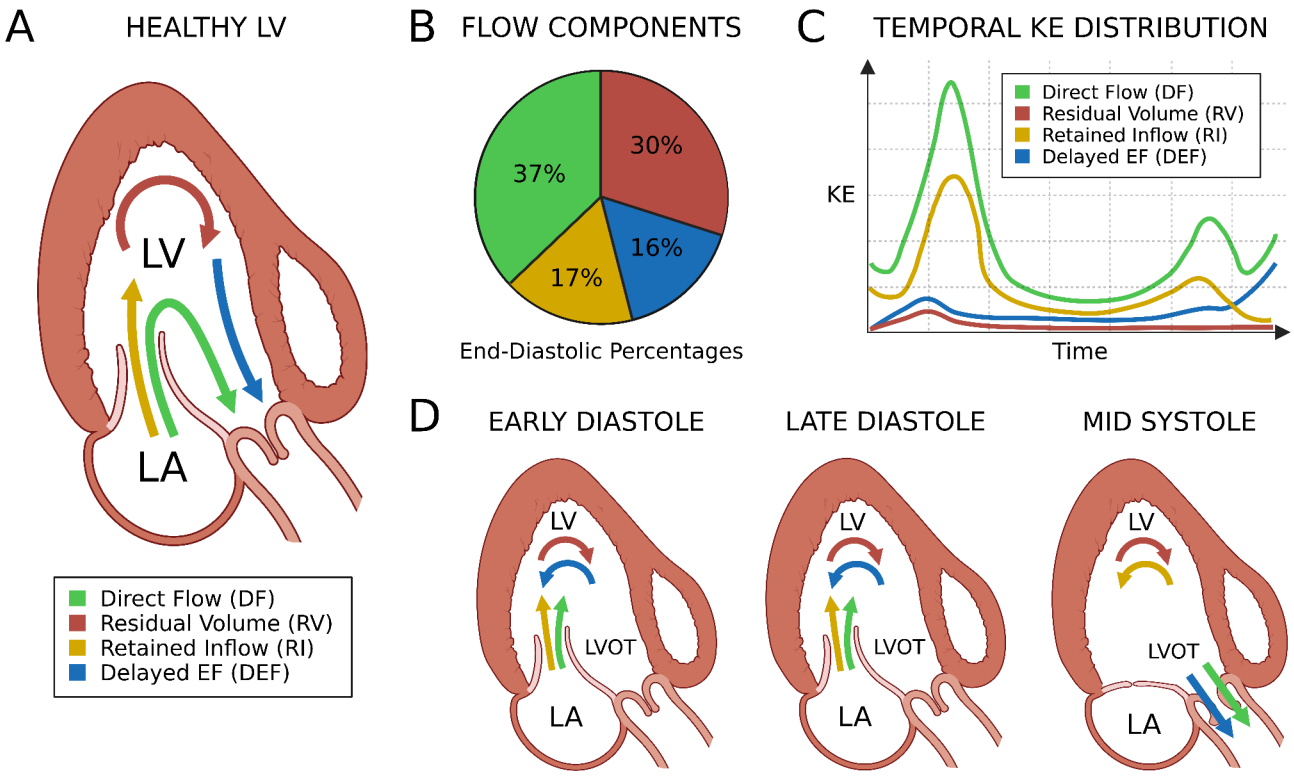

Fig. 4 Illustration of blood flow components inside the left ventricle (LV) cavity of a normal subject. (**A**) The 4 components of the LV end-diastolic volume (EDV) are represented using different colors: direct flow (DF) in green, retained inflow (RI) in yellow, residual volume (RV) in red and delayed ejection flow (DEF) in blue. (**B**) The pie chart shows the normal percentage of the 4 components of the LV EDV. (**C**) The graph illustrates the temporal distribution of blood kinetic energy (KE) for each of the 4 components of the LV EDV. (**D**) Motion of the 4 components of the LV EDV is illustrated at different times during the cardiac cycle

wider, and rounder compared to healthy controls. Additionally, the vortex was sustained throughout the entire cardiac cycle, from the diastolic period to the entire systolic period. This latter observation was corroborated by Zhang et al. [32], who also reported a more apical position of the vortex in patients with reduced LV-EF. Such vortex morphology is disadvantageous, as it does not facilitate the redirection of blood flow toward the LVOT.

Mangual et al. [18] found LV KED to be lower in patients with dilated cardiomyopathy (DCM) than in healthy subjects. Mangual et al. [18] speculated that this reflects an alteration in intraventricular flow transit in DCM patients, indicating a lack of flow redirection toward the LVOT, thus necessitating additional myocardial work to direct blood toward the aorta.

Agati et al. [20] evaluated a group of patients after acute myocardial infarction (MI) with varying LV-EF values, comparing them with normal subjects. In patients with significant LV dysfunction, global KE dissipation indices (relative to the entire cardiac cycle) were markedly reduced due to low flow KE. Conversely, patients with preserved LV-EF showed a significant increase in global KE dissipation indices compared to controls, suggesting the presence of a new fluid-tissue dynamical balance as a compensatory mechanism for maintaining adequate LV-EF. These data were confirmed by Chan et al. [33] using phase-contrast MRI.

Fukuda et al. [34] examined patients with reduced LV-EF, including 29 patients with DCM and 31 with a history of MI. Unlike normal subjects, patients with reduced LV-EF exhibited a persistent vortex throughout the IVCT, the ejection period, and sometimes even into the isovolumetric relaxation time (IVRT). Notably, the persistence of the vortex correlated directly with the degree of LV dilation and the extent of LV-EF reduction. These findings align with those reported by Hong et al. [31] and Zhang et al. [32].

Bermejo et al. [14], in patients with non-ischemic DCM, observed that the main vortex was larger and stronger, even when adjusted for LV size. In most patients, the diastolic vortex ring remained strong at the onset of the A-wave, and the late filling jet did not disrupt it but rather reinforced it. Consequently, the strengthened diastolic vortex maintained its position near the apex.

Kim et al. [35] studied patients with compensated HF and reduced LV-EF, reporting various vortex indices without a comparison group. While vortex length index

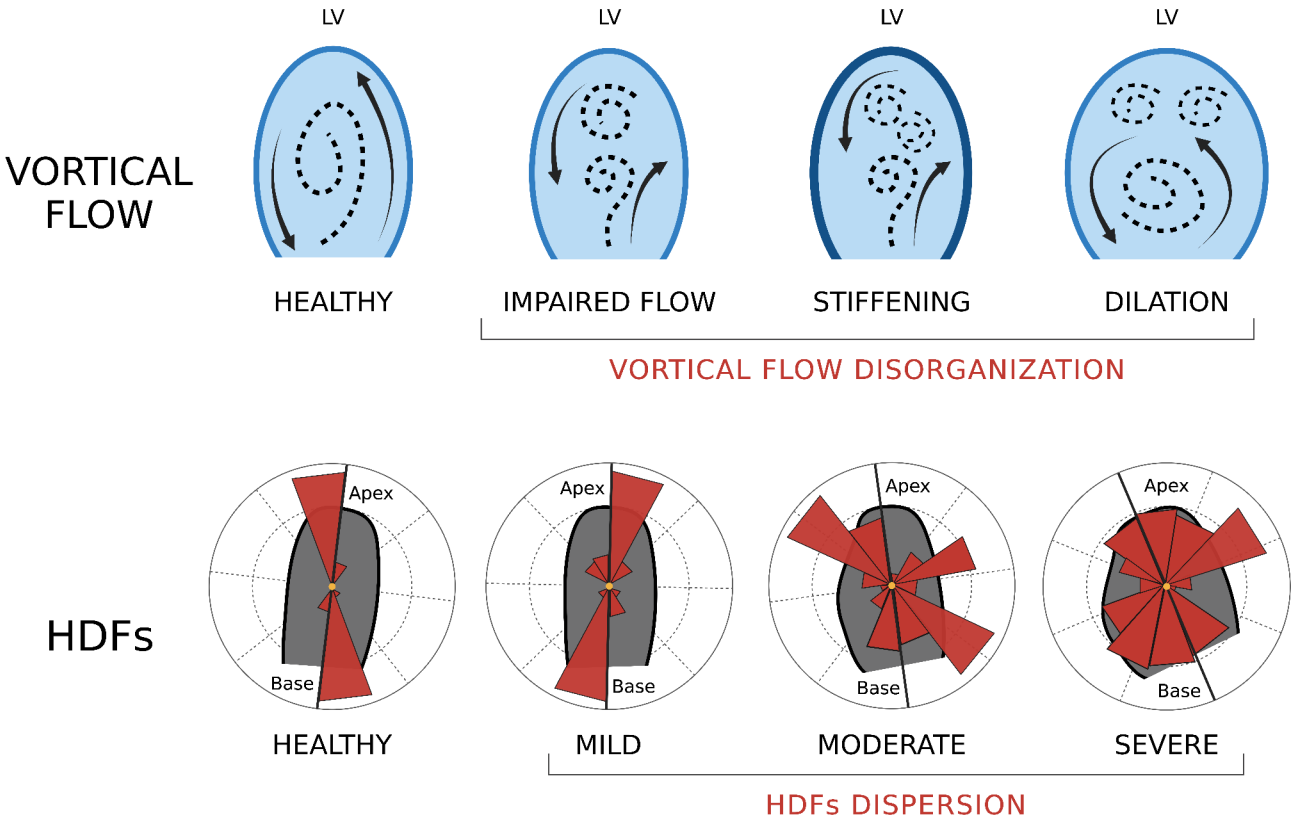

Fig. 5 Top line: different stages of left ventricle (LV) remodeling compared to a normal LV. Bottom line: intensity-weighted polar histograms representing the distribution and intensity of the LV hemodynamic forces (HDFs) occurring during an entire heartbeat

values were lower than those observed in normal subjects in other studies [20, 36], vortex depth index values were similar or slightly higher. Vortex width index values were elevated compared to those reported by Hong et al. [31]. The KED and KEF index values were also lower than those seen in normal subjects in other investigations [20, 36].

Tang et al. [37] compared patients with DCM to healthy subjects, finding that in the DCM group, the vortex area, length, depth indices, and KED index were significantly higher, whereas the flow force angle was significantly lower. However, the flow force angle in normal subjects was unexpectedly high (35.896° ± 6.044°), raising questions about the validity of the comparison with DCM patients.

Fiorencis et al. [5] evaluated patients with stabilized chronic HFrEF. Compared to healthy subjects, HF patients exhibited greater vortex area, length, depth, and intensity indices, but a smaller KED index (Fig. 7). These results were similar to those of Tang et al. [37] regarding vortex geometry indices but differed for the KED index.

Chan et al. [38] studied HFrEF patients and normal subjects. The EDV-indexed E-vortex and A-vortex areas in HFrEF patients were lower than in normal participants. Both the E-vortex and the A-vortex were located more apically in HFrEF patients, as reported by Bermejo et al. [14]. The authors also observed a fragmented vortex pattern in HFrEF patients, which correlated with higher KEL; they hypothesized that vortex fragmentation could contribute to lower energy efficiency, particularly during diastole.

Gharib et al. [39], in a small cohort of DCM patients with impaired LV-EF, reported that the VFT consistently fell below the optimal range. These observations were corroborated by Bermejo et al. [14], Mangual et al. [18], and Agati et al. [20]. Poh et al. [40], using the adapted VFT, reported different mean values compared to Gharib et al. [39] in subjects with structurally normal hearts. However, similar to Gharib et al. [39], the adapted VFT was reduced in HFrEF patients, as well as in HFpEF patients, although to a lesser extent in the latter case.

Overall, these echocardiographic studies demonstrate that vortex flow analysis can effectively differentiate normal subjects from HFrEF patients, utilizing various parameters (i.e., vortex area, length, width, depth, KED/KEL, KEF, VFT, etc.). However, there is some conflicting evidence regarding vortex characteristics in LV dysfunction. These discrepancies may be attributed to differences in ultrasound techniques, chance variations due to small

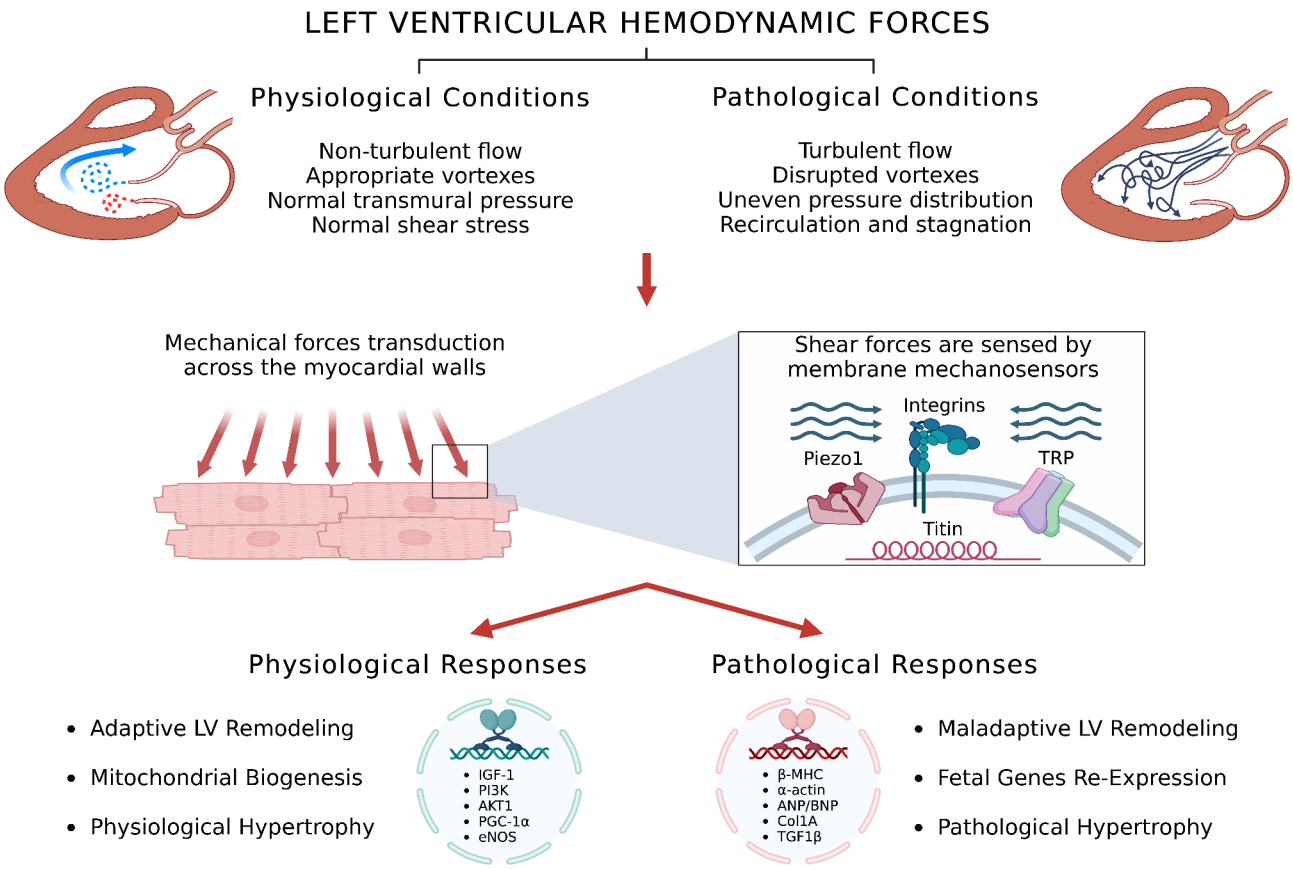

Fig. 6 Physiological and pathological responses to left ventricular (LV) hemodynamic forces. ANP: atrial natriuretic peptide. BNP: brain natriuretic peptide. Col1A: collagen type I alpha. eNOS: endothelial nitric oxide synthase. IGF-1: insulin like growth factor. PGC-1α: peroxisome proliferator-activated receptor-gamma coactivator. PI3K: phosphatidylinositol 3-kinase. β-MHC: myosin heavy chain. TGF1β: transforming growth factor 1β. TRP: transient receptor potential

sample sizes, or variations in how the clinical features of the patients were defined.

4D-Flow MRI studies. Results of the 4D-flow MRI studies are summarized in Table 3.

Initially, Bolger et al. [16] studied a single patient with DCM and reduced LV-EF, showing a reduction in DF and KE at end-diastole, accompanied by an increase in the KE of the retained inflow. Subsequently, Eriksson et al. [17] evaluated another single patient with DCM and reduced LV-EF, reporting findings similar to those of Bolger et al. [16]. Two years later, Eriksson et al. [41] studied a number of patients with DCM, systolic dysfunction, and compensated HF, along with healthy subjects with equivalent SV. They found that the proportion of DF was smaller in DCM patients, although the end-diastolic KE per milliliter of DF was not significantly different between the two groups. In other words, while SV in compensated HF patients with DCM was similar to that of healthy controls, the composition of the SV differed, with a smaller proportion of DF.

Kanski et al. [42] demonstrated that, in HFrEF patients, the average systolic KE was higher compared to controls, while there were no differences in diastolic average KE. Furthermore, three distinct KE time curve patterns were identified in HF patients, all markedly different from those observed in controls. These KE time curves did not correlate with New York Heart Association (NYHA) classification or the 6-minute walk test, leading the authors to suggest that these curves could represent a new method for quantifying HF.

Svalbring et al. [43] studied patients with chronic ischemic heart disease who had NYHA class I and II, with no to mild LV systolic dysfunction and remodeling. They found that the proportions of DF volume and KE decreased with increasing LV EDV index and end-systolic volume (ESV) index. The authors suggested that these alterations (a decrease in DF volume and KE at end-diastole) may help detect LV dysfunction even in cases of subtle or subclinical LV remodeling.

Riva et al. [44] evaluated patients with ICM in comparison to normal subjects. In the ICM patients, the diastolic vortex ring at the time of the peak E- and A-wave showed alterations in terms of geometry and energetics. Specifically, at the peak E-wave, the vortex ring was less circular,

Table 2 Left ventricular (LV) vortex and energetic characteristics in patients with systolic dysfunction and heart failure (HF) evaluated by ultrasound techniques

Author	Imaging Technique	Patients	Vortex Characteristics	KE and KEL/KED/KEF
Gharib et al. 2006 [39]	Transthoracic echocardiography	80 pts with no prior information about cardiac health,7 patients with DCM.	VFT in DCM patients (1.5–2.5) lower than optimal range (3.5–5.5) in subjects with normal LV-EF.	Not evaluated.
Hong et al. 2008 [31]	Echo-PIV	15 patients with LV-EF < 40%, 10 normal controls.	Smaller vortex length index (0.366 ± 0.06) and depth index (0.443 ± 0.04) and greater vortex width index (0.209 ± 0.05) compared to normal controls.	Not evaluated.
Poh et al. 2012 [40]	Transthoracic echocardiography	91 HFrEF patients, 39 HFpEF patients, 32 normal controls.	Reduced VFTa in HFrEF patients (1.25 ± 0.55) and HFpEF patients (2.21 ± 0.8) compared to normal controls (2.67 ± 0.8, $P < 0.001$).	Not evaluated.
Mangual et al. 2013 [18]	3D transthoracic echocardiography + blood flow reconstruction	8 patients with DCM, 20 normal controls.	VFT in DCM patients (4.33 ± 0.37) lower than in normal controls (1.49 ± 0.53, $P < 0.001$).	KED index in DCM patients (2.05 ± 1.52) higher than in normal (1.49 ± 0.53, $P < 0.001$).
Agati et al. 2014 [20]	Echo-PIV	34 patients with acute MI in 3 groups (LV-EF > 50%, 30–50%, < 30%), 30 normal controls.	No differences in area, length, depth and intensity indices. VFT and DF lower in patients, with progressive reduction with reduction of LV-EF.	KED and KEF progressively lower with reduction of LV-EF.
Fukuda et al. 2014 [34]	VFM	60 patients with LV-EF 36 ± 11%, 20 normal controls.	Vortex persistent throughout ICT, ejection time, and IRT; persistence proportional to LV dilation and EF reduction.	Not evaluated.
Bermejo et al. 2014 [14]	Custom-developed color Doppler-based technique	61 patients with NIDCM, 61 normal controls.	Larger vortices in NIDCM. Reduced VFT in NIDCM compared to normal controls (1.43 ± 0.83 vs. 3.95 ± 1.78, $P < 0.0001$). Stronger vortex in NIDCM patients compared to normal controls (circulation: 0.008 ± 0.007 m^2/s vs. 0.006 ± 0.005 m^2/s, $P = 0.02$).	Higher KE in NIDCM patients compared to normal controls (7 ± 8 mJ/m vs. 5 ± 5 mJ/m, $P = 0.04$).
Kim et al. 2018 [34]	Echo-PIV	75 patients with HF and LV-EF ≤45%.	Average vortex length index 0.53–0.54, depth index 0.39–0.42, width index 0.32.	Average KED index: 0.32–0.33. KEF index: from 0.71 ± 0.2 to 0.92 ± 0.38 depending on MACE.
Tang et al. 2018 [37]	Echo-PIV	20 patients with DCM, 20 normal controls.	In the DCM group, higher vortex area (0.237 ± 0.063 vs. 0.196 ± 0.129, $P = 0.029$), vortex depth (0.396 ± 0.134 vs. 0.293 ± 0.143, $P = 0.025$), and vortex length (0.534 ± 0.089 vs. 0.435 ± 0.176, $P = 0.004$); flow force angle significantly lower (29.979 ± 8.208 vs. 35.896 ± 6.044, $P = 0.013$).	In the DCM group, higher KED (0.975 ± 0.552 vs. 0.578 ± 0.295, $P = 0.006$).
Fiorencis et al. 2022 [5]	HyperDoppler	47 patients with LV-EF < 50%, 50 normal controls.	Greater vortex area index (0.31 ± 0.04), length index (0.73 ± 0.08), depth (0.39 ± 0.06) compared to normal controls.	Greater intensity index (-0.42 ± 0.04) and smaller KED index (0.19 ± 0.09) compared to normal controls.
Chan JSK et al. 2023 [38]	VFM	20 patients with HFrEF, 20 normal controls.	In HFrEF patients, greater vortex S-area index (2.73 ± 1.19 mm^2/ml), E-area index (3.03 ± 1.23 mm^2/ml) and A-area index (3.22 ± 1.23 mm^2/ml) compared to normal controls.	In HFrEF patients, greater mean EL_D (3.99 ± 2.14 10^{-2} J/ms) and peak EL_E (8.66 ± 6.27 10^{-2} J/ms) compared to normal controls.

3D: three-dimensional. DCM: dilated cardiomyopathy. DF: direct flow. Echo-PIV: echocardiographic particle image velocimetry. EL_D: diastolic energy loss. EL_E: energy loss at the time of the E wave. HFpEF: heart failure preserved ejection fraction. HFrEF: heart failure reduced ejection fraction. KE: kinetic energy. KED: kinetic energy dissipation. KEF: kinetic energy fluctuation. KEL: kinetic energy loss. ICT: isovolumetric contraction time. IRT: isovolumetric relaxation time. LV-EF: left ventricular ejection fraction. MACE: major adverse cardiovascular event. MI: myocardial infarction. NIDCM: non-ischemic DCM. VFM: vector flow mapping. VFT: vortex formation time; VFTa: adapted vortex formation time

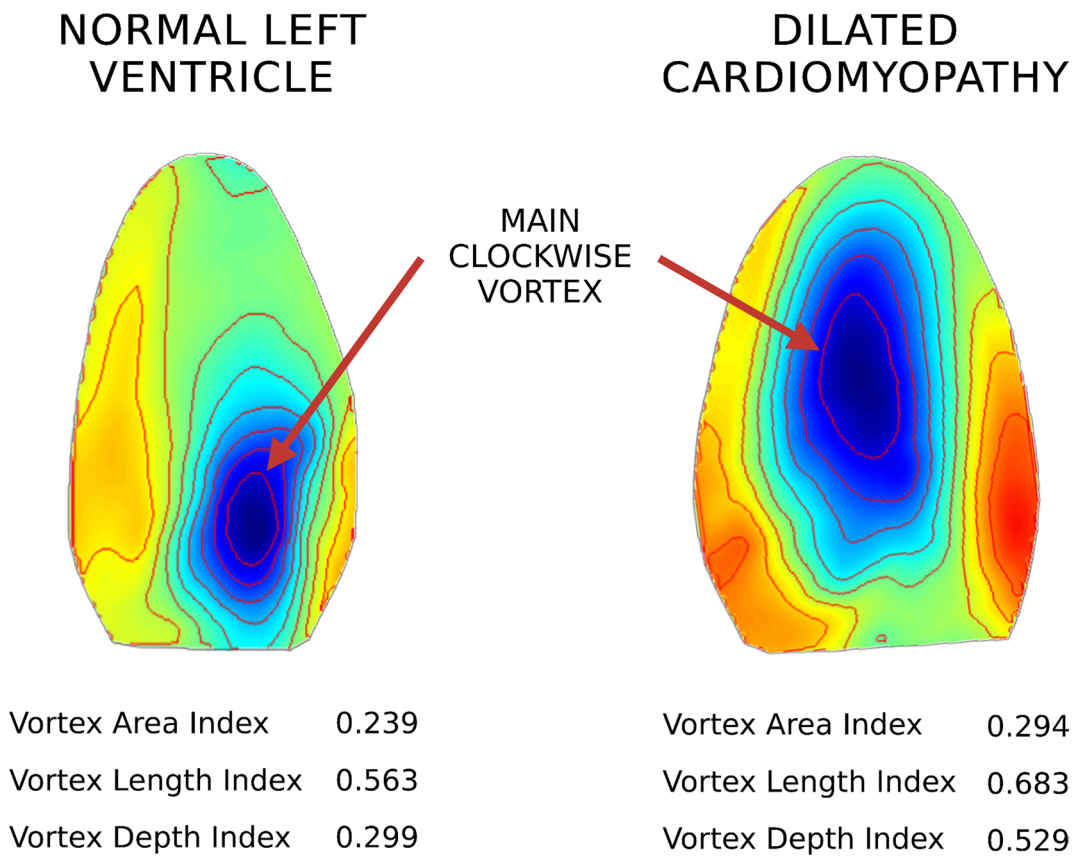

Fig. 7 Examples of steady-streaming flow images of the left ventricle of a normal subject and a patient with dilated cardiomyopathy. The steady-streaming flow field evaluates the overall circulatory pattern in the left ventricle during one heartbeat. Images were obtained using the HyperDoppler technique (modified from reference [5]). Geometrical measures of the main vortex are reported

Table 3 Left ventricular (LV) vortex and energetic characteristics in patients with systolic dysfunction and heart failure (HF) evaluated by 4D-flow magnetic resonance imaging (MRI)

Author	Imaging Technique	Patients	Vortex Characteristics	KE and KEL/KED
Bolger et al. 2007 [16]	4D-flow MRI	Single patient with DCM and LV-EF 31%, 17 normal controls.	Reduced end-diastolic DF.	Reduced end-diastolic KE.
Eriksson et al. 2011 [17]	4D-flow MRI	Single patients with DCM and LV-EF 35%, 13 normal controls.	Reduced DF.	Reduced late-diastolic KE of DF.
Eriksson et al. 2013 [41]	4D-flow MRI	10 patients with DCM and LV-EF 42 ± 5%, 10 normal controls.	Reduced DF compared to normal controls (20 ± 5% vs. 38 ± 5%, $P < 0.0125$).	End-diastolic KE per ml of DF similar to normal controls.
Kanski et al. 2015 [42]	4D-flow MRI	29 HF patients (62% with IHD) with LV-EF 26 ± 8%, 8 normal controls.	Non reported.	Higher systolic KE compared to normal controls (2.2 ± 1.4 mJ vs. 1.6 ± 0.6 mJ, $P = 0.048$), no difference in diastolic KE (3.2 ± 2.3 mJ vs. 2.0 ± 0.8 mJ, $P = 0.13$).
Svalbring et al. 2016 [43]	4D-flow MRI	26 patients with chronic IHD with no-to-mild LV systolic dysfunction, 10 normal controls.	DF reduced with increasing LV EDV index and ESV index (r =-0.64 and r = -0.74, both $P < 0.001$).	DF KE reduced with increasing LV EDV index and ESV index (r = -0.48, $P = 0.013$, and r = -0.56, $P = 0.003$).
Riva et al. 2024 [44]	4D-flow MRI	15 patients with ICM, 15 normal controls.	Vortex ring less circular at peak E-wave ($P = 0.032$) and more circular at peak A-wave ($P = 0.034$) in ICM patients.	At both peak E-wave and peak A-wave, vorticity index, KE index and rate of viscous EL index significantly decreased in ICM patients.

DCM: dilated cardiomyopathy. DF: direct flow. EDV: end-diastolic volume. ESV: end-systolic volume. KE: kinetic energy. KED: kinetic energy dissipation. KEL: kinetic energy loss. EL: energy loss. ICM: ischemic cardiomyopathy. IHD: ischemic heart disease. LV-EF: left ventricular ejection fraction

while at the peak A-wave, the circularity index was significantly increased compared to normals. The KE and the rate of viscous KEL indexed for the entire LV decreased compared to healthy controls.

Carlhäll and Bolger [45] summarized the findings provided by 4D-flow MRI with the analysis of LV blood flow components in failing hearts. They pointed out that, in general, compensated HF states exhibit less disordered flow than decompensated states, although elevated residual volume and impaired KE conservation remain. According to Carlhäll and Bolger [45], analysis of LV blood flow components can be helpful in recognizing HF patients, both in advanced and moderate stages of the disease, as well as in cases of mild/subtle or subclinical LV remodeling. Decreases in DF and KE at end-diastole are considered to be the best markers for identifying LV systolic dysfunction.

Diastolic dysfunction. LV diastolic dysfunction is a major cause of HF syndrome, both in HFrEF and in HFpEF. As previously mentioned, when the LV actively relaxes and expands during diastole, it generates a pressure gradient and KE, facilitating LV filling from the left atrium. However, not all the KE generated by myocardial relaxation is converted into blood flow KE. Some of it is lost as viscous EL — the KE lost as heat due to the friction of blood against the ventricular walls — while part of it is dissipated as turbulent KE, which is lost in the form of small turbulent eddies.

Indices of KE dissipation are expected to vary with changes in diastolic filling. Additionally, the HDFs (those exerted by the intraventricular blood flow on the myocardium, derived from the IVPGs), should also be considered. Indeed, alterations in the direction and magnitude of these HDFs can reflect disturbances in blood flow caused by impaired diastolic filling [46].

Echocardiographic studies. A number of studies using VFM have shown that LV KEL can identify patients at potential risk of HF when comorbidities such as diabetes mellitus [47, 48], chronic kidney disease [49–51], and hypertension [49] are present. In particular, Zhong et al. [50] observed that patients undergoing dialysis exhibit greater systolic and diastolic LV KEL compared to healthy individuals, despite having comparable LV-EFs. Wang et al. [51] demonstrated that in patients with chronic renal failure (some of whom on dialysis), KEL levels increase. Chen et al. [49] reported that poorly controlled hypertension is a critical contributor to intracardiac blood flow abnormalities in patients with chronic renal failure. Overall, the results from these studies indicate that KEL may serve as a potential predictor of HF by facilitating the early identification of individuals with diastolic dysfunction and increased LV filling pressure. Moreover, KEL can differentiate between various LV filling patterns, as it increases with the severity of diastolic dysfunction [51], particularly in patients with pseudonormal and restrictive filling phenotypes [52].

Additional parameters have been proposed in other studies to recognize different levels of LV diastolic dysfunction [53–55]. Han et al. [53] observed a significant relationship between patterns of LV isovolumic relaxation flow (IRF), which is the flow that occurs in the LV during the IVRT, and LV filling patterns. Berlot et al. [54] studied 121 subjects with normal LV-EF and varying degrees of diastolic dysfunction. The apical intraventricular velocity gradient was able to discriminate between groups with different levels of diastolic dysfunction and was closely associated with classical echocardiographic indices of elevated LV filling pressure. Kheradvar et al. [55] evaluated 107 subjects with different patterns of transmitral diastolic filling and observed that patients with varying patterns of transmitral diastolic filling differed significantly in LV volume filling time.

Unfortunately, these parameters (KEL, IRF, apical intraventricular velocity, volume filling time) have not been compared in the same patients, so their relative accuracy remains unknown.

4D-flow MRI studies. Studies conducted using 4D-flow MRI have examined LV diastolic flow dynamics primarily in patients with HF and left bundle branch block (LBBB) [56–58].

Eriksson et al. [56] reported that LV HDFs in HF patients with LBBB were more orthogonal to the main LV flow direction during early diastole compared to patients without LBBB, although this discrepancy was not observed in late diastole.

Arvidsson et al. [57] calculated the diastolic force ratio, which is the ratio of transverse (lateral-septal and inferior-anterior) to longitudinal (apical-basal) HDFs during diastole in HF patients with reduced LV-EF and LBBB. Their findings revealed reduced longitudinal forces and increased transverse forces in HF patients compared to controls. The diastolic force ratio effectively distinguished healthy from diseased LVs.

Zajac et al. [58] investigated the impact of mechanical dyssynchrony on diastolic function in HF patients with ischemic and non-ischemic cardiomyopathy, both with and without LBBB. Although diastolic flow volume was comparable between groups, the KE at end-diastole was lower in patients with LBBB.

Other studies explored different approaches to studying LV diastolic dysfunction. For example, Toger et al. [59] calculated vortex-ring mixing during LV early filling as a potential index of diastolic dysfunction and HF. The underlying concept is that vortex-ring rotation generates a mixing of inflowing fluid (from the left atrium) and surrounding fluid present in the LV. This mixing was expressed through different parameters, which demonstrated good performance in distinguishing controls from

HF patients with reduced LV-EF. However, no differences in mixing parameters were observed among patients with different classes of diastolic dysfunction.

Collectively, the results of these studies indicate that diastolic HDF and KE measures (diastolic force ratio, end-diastolic KE) obtained using 4D-flow MRI are markers of LV mechanical dyssynchrony in HF patients with LBBB. However, this MRI technique has both strengths and limitations in diagnosing LV diastolic dysfunction [60]. One limitation is that 4D-flow MRI is generally not performed in routine clinical practice.

Recently, conventional cine MRI has been proposed for estimating LV HDFs [61]. This approach has been validated against 4D-flow MRI, providing an opportunity to include the evaluation of LV HDFs in clinical MRI applications.

Lapinskas et al. [62] analyzed HDFs in patients with HFpEF, HFrEF and HF with mildly reduced EF (HFmrEF). They found that LV longitudinal HDF was significantly decreased in patients with HFpEF compared to healthy controls, while no differences were observed in LV-EF, global longitudinal strain, or global circumferential strain between the groups. However, other authors did not find any differences in HDF parameters between HFpEF patients and healthy controls [63].

Backhaus et al. [64] studied 34 patients with HFpEF and 34 with non-cardiac dyspnea, based on pulmonary capillary wedge pressure values obtained during cardiac catheterization. Patients with HFpEF exhibited lower LV longitudinal HDF compared to those with non-cardiac dyspnea.

Airale et al. [65] performed a retrospective study evaluating HDFs in 67 patients, of whom 33 (49%) had increased LV filling pressure. The diastolic longitudinal HDF, reflecting the mean amplitude of LV longitudinal HDF during diastole, was associated with the presence of increased LV filling pressure.

Overall, these studies highlight the potential of HDFs obtained using conventional MRI for evaluating HFpEF in clinical practice. However, this approach requires further validation, as some investigators reported conflicting results [63].

LV flow dynamics and thrombosis

The normal LV flow pattern allows for complete washing of the LV in about 2 to 4 beats without inducing shear values high enough to activate platelets. In patients with ICM, particularly those with anterior MI or non-ischemic DCM characterized by diffuse LV hypokinesis, physiological blood flow patterns are disrupted. This disruption may lead to blood stasis or abnormally high shear stresses, increasing the risk of LV thrombosis (Fig. 8).

Ischemic heart disease. Son et al. [66] utilized the echo-PIV technique in patients with acute anterior MI and highlighted that reduced vortex depth was strongly associated with the formation of apical LV thrombus.

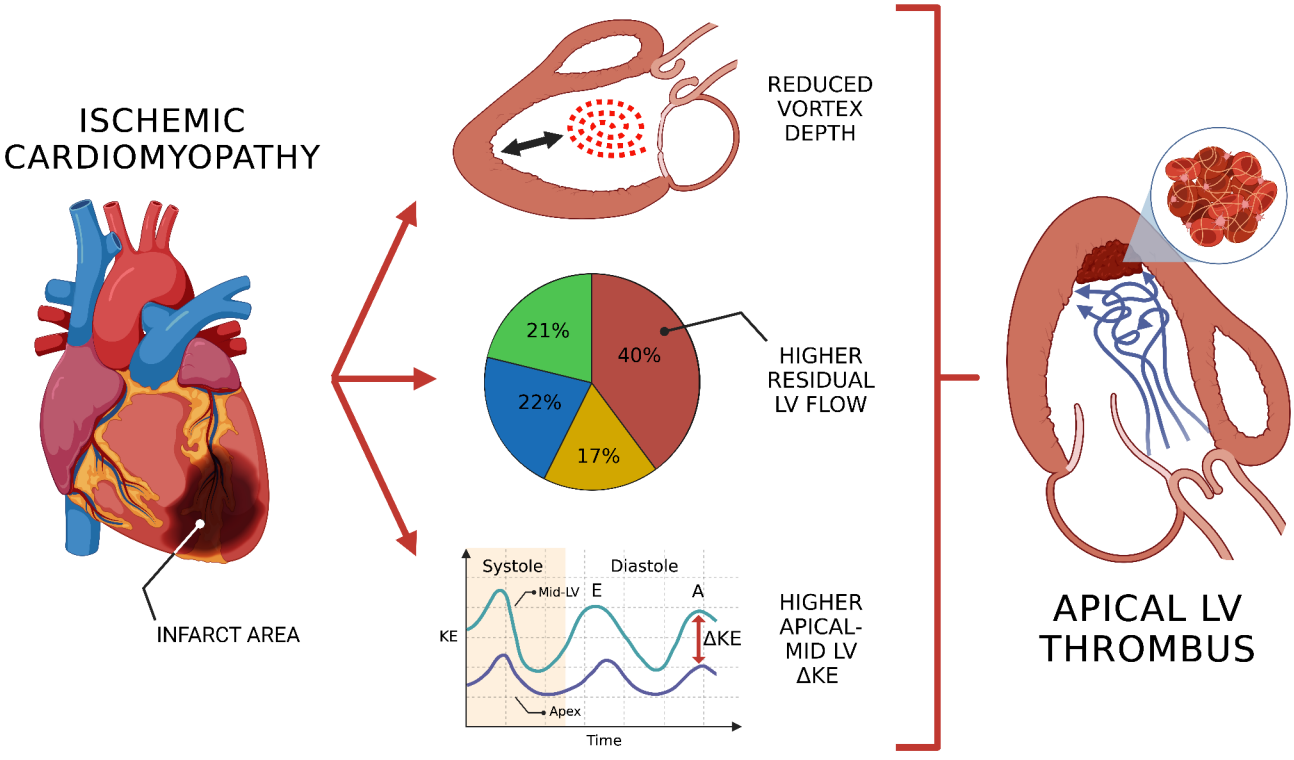

Fig. 8 Factors relative to abnormal flow dynamics which favor development of apical thrombosis of the left ventricle (LV). KE: kinetic energy

Notably, a vortex depth index of < 0.45 remained a significant independent parameter for the formation of the apical LV thrombus.

Devesa et al. [67], in a pilot study involving 28 patients with acute anterior MI, employed a methodology for the quantitative and topological assessment of flow residence time within the LV based on color Doppler velocities. Patients with thrombosis exhibited a higher proportion of LV blood volume with flow residence time > 1 beat (72 ± 3% vs. 47% ± 15%, $P < 0.001$) and a lower normalized apical position of retained blood (0.59 ± 0.06 vs. 0.71 ± 0.11; $P = 0.04$).

Garg et al. [68] conducted a prospective cohort study using 4D-flow MRI in both acute and chronic MI patients (MI > 3 months). They found that MI patients had reduced global LV flow KE. Furthermore, MI patients with LV thrombus demonstrated a decrease in apical A-wave KE, which represents the late diastolic wash-in of the distal LV.

Demirkiran et al. [69], employing 4D-flow cardiac MRI in chronic MI patients with LV thrombus, provided evidence of altered LV flow dynamics, including abnormal diastolic vortex ring geometry, disrupted vorticity vector fields, and irregular distributions of flow components.

Sakakibara et al. [70] applied 4D-flow MRI to patients with various types of cardiac disease, including 50% with ICM and LV-EF ≤ 40%. They found that a smaller LV vortex and lower flow velocity at the LV apex were associated with the presence of LV thrombus.

Dilated cardiomyopathy. Blood transport is significantly altered in patients with non-ischemic DCM [14]. In these patients, blood is trapped within strong, long-lasting vortices that undergo rotation throughout most of the cardiac cycle, during which blood is continuously exposed to shear forces. Rossini et al. [71] observed in 20 patients with DCM the presence of a clockwise vortex with higher circulation compared to healthy controls (median 99 cm^2/s vs. 60 cm^2/s, $P = 0.007$). They also noted increased indices of LV stasis, including a higher average residence time T_R (median 1.9 s vs. 1.4 s, $P < 0.001$) and a greater area of regions with $T_R > 2$ s (median 40.7% vs. 27.1%, $P = 0.003$). Platelet activation and stasis may explain the increased risk of thrombosis in patients with DCM.

In summary, although the mechanisms underlying thrombus formation are multifaceted, advanced vortex imaging has the potential to identify some of these mechanisms and high-risk patients, paving the way for optimized anticoagulation strategies and improved outcomes in ICM.

Secondary mitral regurgitation

Secondary mitral regurgitation (MR) due to LV dysfunction, also known as functional MR, is associated with significant morbidity and mortality in patients with HF. Both experimental and clinical evidence indicates that MR significantly alters intracardiac flow dynamics and alterations may vary substantially between secondary and primary MR [4]. In severe secondary MR, flow studies typically revealed unstructured vortices with a dominant clockwise rotation, elevated KED, and an absence of a clear ring vortex during diastolic inflow. By contrast, degenerative MR exhibit more heterogeneous patterns, also influenced by the presence of prolapse. These findings underscore that while both primary and secondary MR can disrupt normal vortex formation, the specific flow signatures —such as vortex orientation, energy dissipation, and velocity profiles— are etiology-dependent and may accelerate LV remodeling through the same aforementioned cellular and molecular mechanisms. Ultimately, the progressive remodeling and altered hemodynamics in these patients can drive or exacerbate HF if left untreated.

LV flow dynamics for HF treatment

Modifications of LV flow dynamics have been described across HF treatments, including pharmacological therapy, cardiac resynchronization therapy (CRT), and left ventricular assist devices (LVADs).

Pharmacological therapy. Although there are no extensive multicenter studies utilizing intracardiac flow dynamics to guide pharmacological therapy in HF, initial observations have been published.

Nabeta et al. [72] used 4D-flow MRI to document the effects of medical therapy on a single patient with DCM and severely reduced LV-EF (18%).

Monosilio et al. [73], in a study on 50 patients with HFrEF conducted utilizing echocardiography, observed that sacubitril/valsartan induced LV reverse remodeling, leading to increased myocardial contractility and improved HDF distribution. Specifically, after 6 months of therapy, indexed LV volumes decreased, LV-EF and global longitudinal strain improved, and a realignment of HDFs occurred, with a reduction in the diastolic ratio between transversal and longitudinal HDFs (23% vs. 20%; $P < 0.001$).

In another echocardiographic study, Fabiani et al. [74] evaluated the predictive value of HDFs on the 6-month treatment response to sacubitril/valsartan in 89 HFrEF patients. Patients were categorized as responders if they did not experience any adverse events and exhibited a reduction of at least 50% in N-terminal pro–B-type natriuretic peptide (NT-proBNP) and/or an increase of 10% or more in LV-EF over 6 months. Only LV longitudinal HDF differed significantly between responders and

non-responders, being higher in responders (4.4% vs. 3.6%; $P = 0.01$). LV longitudinal HDF was the only independent predictor of response to sacubitril/valsartan in multivariable logistic regression analysis [OR 1.36; 95% confidence interval 1.10–1.67].

These preliminary studies suggest that HDF analysis has the potential to optimize decision-making in patients with HFrEF. According to Carlhäll and Bolger [45], other metrics of flow dynamics, such as reductions in LV residual volume and KEL, might also serve as markers of therapeutic response.

Cardiac resynchronization therapy and multipoint pacing. Applications of LV flow dynamics analysis—primarily conducted using ultrasound techniques—to patients undergoing CRT have been reviewed elsewhere [6, 12, 75].

Some studies have evaluated the effects of CRT activation and deactivation on LV flow dynamics and the associated blood flow behavior in relation to CRT response. Initially, Goliasch et al. [76] observed that CRT deactivation delayed the onset of the diastolic vortex, prolonging the redirection of blood flow towards the aorta and thus perpetuating a delay in the IVCT. Upon CRT reactivation, there was an acute restoration of LV diastolic vortex formation, which immediately improved LV filling, optimizing the timing of diastolic vortex formation and shortening the IVCT.

Pedrizzetti et al. [77, 78] found that switching off CRT resulted in a loss of alignment of the LV HDFs and the development of transversal components, even though cardiac contractility and synchrony parameters showed no measurable changes. In CRT non-responders, flow alignment was absent both when the pacemaker was active and when it was switched off.

Cimino et al. [79] demonstrated that in CRT responders with CRT turned off, KED was lower, indicating the formation of a more compact and uniform LV vortex. Conversely, in CRT non-responders with CRT off, KED was higher and "paradoxically" increased when CRT was activated, alongside an increase in LV dyssynchrony, a lack of variation in LV-EF and a more chaotic and non-uniform vortex formation.

In recent years, several authors have applied the analysis of HDFs based on speckle tracking echocardiography to study patients undergoing CRT. Examples of LV HDF patterns are illustrated in Fig. 9. Dal Ferro et al. [80] found that among patients implanted with CRT, those who exhibited improved alignment of HDFs immediately after the CRT implant had a higher rate of response at follow-up. Laennens et al. [81] reported, as expected, that the magnitude of HDFs was significantly lower and the orientation significantly worse in patients with HF compared to healthy controls. Immediately following CRT implantation, the apical-basal impulse and the angle of the systolic force vector were significantly increased, and this improvement persisted 6 months post-CRT. When CRT was deactivated at 6 months, the increase in the magnitude of apical-basal HDF remained unchanged, while the angle of the systolic force vector deteriorated significantly. In a subsequent study, Laennens et al. [82] observed that the orientation of the HDF at baseline was associated with LV response to CRT. Specifically, 6 months after CRT, the orientation of HDFs improved in both LV responders and non-responders, while the magnitude of the apex-base HDF only improved in LV responders.

Some authors have used HDFs obtained through 4D-flow MRI to identify patients who are unlikely to benefit from CRT. Specifically, Pola et al. [83] evaluated HDFs in 22 HF patients with an LV-EF < 35% and LBBB at baseline and again 6 months after CRT. Non-responders exhibited smaller diastolic longitudinal HDF during filling and a higher diastolic force ratio (0.89 vs. 0.67; $P = 0.004$) compared to responders. A diastolic force ratio > 0.87 identified CRT non-responders with 57% sensitivity and 100% specificity (AUC 0.88; $P = 0.005$).

Siciliano et al. [84] observed that multipoint pacing led to better realignment of LV HDFs compared to standard biventricular pacing in HF patients. This resulted in a significant reduction in LV EDV and ESV compared to conventional CRT.

Finally, other studies have attempted to determine whether flow dynamics analysis can influence or guide CRT optimization. Muñoz et al. [85, 86], using non-contrast color Doppler-based analysis of intracardiac flows, found that optimal atrioventricular delay in CRT promotes physiological vortex flow patterns in the LV during the end-diastolic and early systolic periods. These patterns are disrupted when non-optimal values are programmed, leading to increased KED.

Left ventricular assist devices. LVADs are mechanical pumps that are surgically connected to the LV and aorta, designed to increase aortic flow and end-organ perfusion. The success of LVAD therapy is hampered by complications, including thrombosis and bleeding, which are related to abnormalities in blood flow dynamics induced by the device [87, 88] (Fig. 10).

It should be noted that the LVAD forces the LV to function primarily as a conduit, while the native LV alternates between reservoir function (during diastole) and booster function (during systole). The continuous suction from the LVAD cannula generates a strong mitral jet that extends from the base of the LV to the apex and persists throughout the entire cardiac cycle. Consequently, LVAD treatment redirects blood flow through the LV, creating a straight channel between the mitral valve and the LVAD cannula located at the LV apex, rather than following a curvilinear path through the LV inflow tract, the main LV

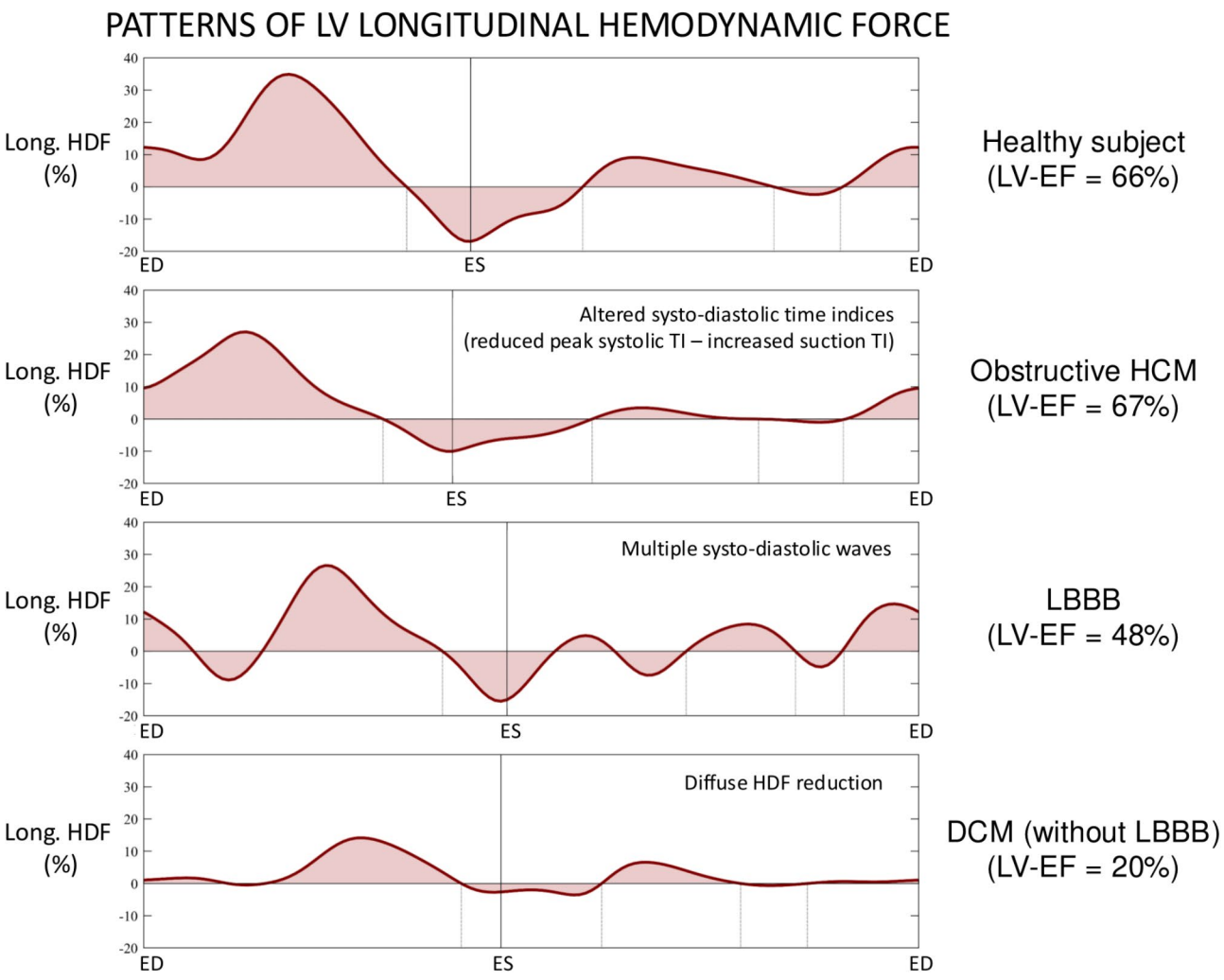

Fig. 9 Different patterns of longitudinal hemodynamic forces (HDFs) within the left ventricle (LV) cavity. Compared to the normal HDF curve, in the obstructive hypertrophic cardiomyopathy (HCM) there is a reduction of both systolic and diastolic HDFs, with alterations of systolic and diastolic time indices: the systolic time index (TI, time interval to systolic peak) reduces and the suction TI (interval including late systolic deceleration and early diastolic suction) increases. The duration of the systolic LV impulse also decreases. In the left bundle branch block (LBBB), the amplitude of the longitudinal HDFs is maintained but the asynchronous activation of the LV myocardium generates multiple waves in systole and diastole, due to the uncoordinated contraction and relaxation. In dilated cardiomyopathy (DCM) there is a generalized reduction of the longitudinal HDFs. EF: ejection fraction

chamber, and the LVOT. This creates a region with high T_R and KE (with low flow velocities) near the LVOT, leading to blood stasis and providing a hemodynamic explanation for the clinical reports of mural thrombosis in the LVOT of patients with LVADs [89]. Additionally, platelet activation increases the thrombotic risk.

Several in vitro, in silico, and ex vivo models have suggested that pump speed, aortic valve opening, cannula location, and orientation are important determinants of intraventricular flow in patients with LVADs [90]. However, to date, only two studies have been conducted in vivo [71, 91]. These studies utilized ultrasound techniques, as 4D-flow MRI cannot be applied in LVAD patients due to the presence of ferromagnetic components in the device.

Schinkel et al. [91] prospectively studied 17 patients who had received a HeartMate III LVAD using the echo-PIV technique. These authors were able to measure vortex geometry, vorticity, KE dissipation, and fluctuation indices; however, a control group was not evaluated for comparison, which limits the interpretation of the results.

Rossini et al. [71] applied echocardiographic color Doppler velocimetry (echo-CDV) to 8 patients with LVADs (7 with a HeartMate II and 1 with a HeartMate III), 20 patients with non-ischemic DCM (median LV-EF 28%), and 20 healthy subjects. These authors found that LVAD support significantly decreased the average T_R of blood and reduced blood stasis compared to DCM patients. This effect was attributed to the shorter and straighter

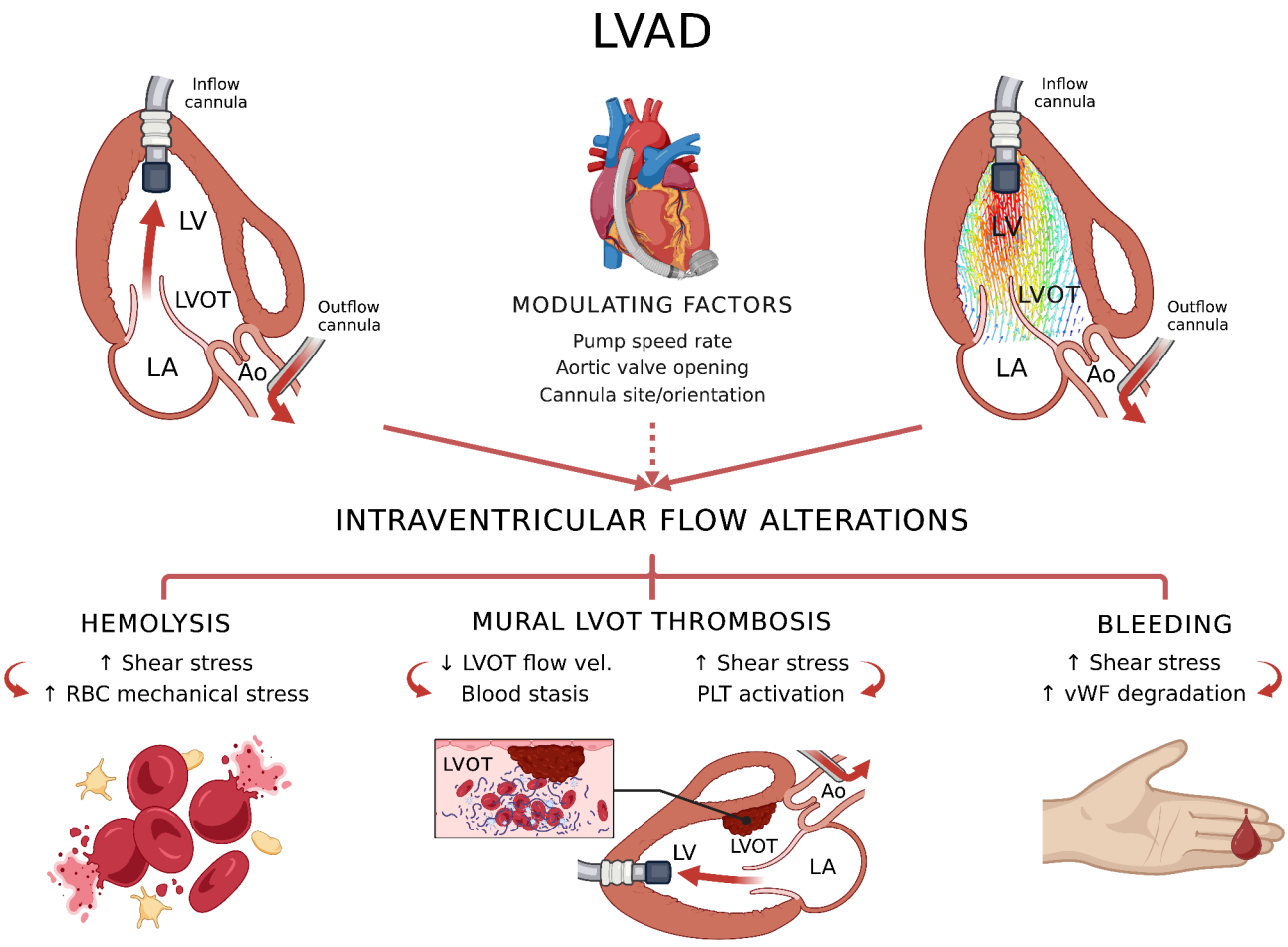

Fig. 10 Factors related to abnormal flow dynamics which favor development of left ventricle (LV) thrombosis, hemolysis and bleeding in patients with left ventricular assist device (LVAD). Modulating factors are also indicated. Ao: aorta. LA: left atrium. LVOT: left ventricular outflow tract. RBC: red blood cell. Vel.: velocity. vWF: von Willebrand factor

route for blood transit within the LV, as described above. However, LVAD treatment generated high instantaneous shear stresses along the edges of the longitudinal inflow jet created by suction at the cannula, which may contribute to platelet activation. Interestingly, LVAD patients with moderate to severe aortic insufficiency exhibited an increase in the average T_R of blood compared to those without aortic insufficiency. This finding relates to the interaction between the aortic regurgitant jet and the mitral inflow jet, which forces intraventricular blood to oscillate back and forth in the LV chamber, thereby impairing LV washout and increasing T_R. The cumulative shear index was also higher in patients with significant aortic insufficiency.

Based on the results of Rossini et al. [71], noninvasive flow imaging could potentially be helpful for adjusting LVAD settings to optimize flow transport and minimize blood stasis and shear indices on an individual basis.

Intracardiac flow dynamics and outcome in HF patients

Because changes in vortex flow characteristics may negatively impact cardiac hemodynamics and function, an influence of alterations in LV flow dynamics on outcomes is expected.

Echocardiographic studies. Different authors, using the echo-PIV technique, have documented the impact of various measures of LV blood flow dynamics on patient outcomes.

Abe et al. [92] followed a small group of 23 patients with HF over a median follow-up period of 2.9 years. Patients who experienced adverse clinical events ($n = 8$) showed a lower change in vortex strength ($P = 0.004$) compared to those who did not experience events ($n = 15$). The difference in vortex strength change between the two groups persisted even after adjusting for differences in LV-EF ($P = 0.03$).

Kim et al. [35] demonstrated that a low KEF is an independent predictor of major adverse cardiac events (MACE), which include cardiac death, heart

transplantation, HF hospitalization, and ventricular tachycardia or fibrillation, during a median follow-up of 277 days. The optimal cut-off value for KEF was determined to be 0.85 based on ROC curve analysis (AUC = 0.653, sensitivity = 0.86, specificity = 0.50, $P = 0.026$). The predictive capability of KEF is understandable because a low KEF indicates low energy capacity in patients with systolic dysfunction and a dilated LV.

Poh et al. [40] found that the adapted VFT calculated using conventional echocardiography independently predicted a composite of adverse events, including cardiovascular death and rehospitalization for HF, during a median follow-up period of 741 days. This observation aligns with the concept that inefficient vortex formation results in suboptimal transfer of KE from diastole to systole. The optimal adapted VFT cut-off value for prediction was 1.32 cm/s (sensitivity 65%, specificity 72%).

Fabiani et al. [74], studying HDFs in patients with HFrEF during a median follow-up of 33 months, documented that an increase in LV longitudinal HDF at 6 months during treatment was an independent predictor of the composite endpoint of HF-related hospitalization, atrial fibrillation, and cardiovascular death (hazard ratio 0.76; $P < 0.001$), after adjusting for clinical and instrumental variables (optimal cut-off value: ≥0.5%; AUC = 0.811).

MRI studies. Backhaus et al. [64] used conventional MRI to evaluate HDFs and found that impairment of systolic peak forces was associated with cardiovascular mortality and hospitalization [hazard ratio 0.95; $P = 0.016$], and it was superior to LV global longitudinal strain assessment in predicting outcomes [AUC 0.76 vs. 0.61; $P = 0.048$].

Stoll et al. [93] assessed 34 patients with DCM, 30 with ICM, and 36 controls using 4D-flow MRI. They found that patients had a reduced proportion of DF and average KE compared to controls ($P < 0.0001$), while the proportion of residual volume and average KE of residual volume were increased ($P < 0.0001$). Importantly, in a multiple linear regression model predicting the patients' 6-minute walking test performance, the independent predictors were age and average KE of DF. In contrast, neither LV-EF nor LV volumes were independently predictive. This independent predictive relationship between average KE of DF and a prognostic measure of functional capacity suggests that analyzing intracardiac flow dynamics may provide additional value in monitoring new therapies and predicting prognosis in HF patients.

Vos et al. [94] reported that, among 168 out of 447 DCM patients, a temporary reversal of the pressure gradient during the systolic–diastolic transition hindered LV diastolic filling. This pressure reversal was found to predict worse outcomes in terms of HF hospitalizations, life-threatening arrhythmias, and sudden cardiac death (hazard ratio 2.57; $P = 0.047$). In cases where pressure reversal was absent, lower LV longitudinal HDF, LV systolic longitudinal HDF, and E-wave deceleration force proved to be powerful independent predictors of the same outcomes.

Gaps in information

There are several unresolved issues regarding LV flow dynamics in the context of HF.

First, most existing information pertains to HFrEF. More studies are needed, particularly focusing on patients with HFpEF, who are often characterized by a normal or even reduced LV cavity size, which may hinder intraventricular vortex development. Additionally, research has predominantly concentrated on the LV, while investigations into the right ventricle and the atria are limited in HF patients. This is especially relevant for diastolic dysfunction, as during diastole the atrioventricular valve is open, connecting the two chambers into a single unit, where the dysfunction of one chamber directly affects the other [46].

Second, it remains unclear whether findings obtained in patients with normal sinus rhythm can be generalized to those with irregular rhythms, such as atrial fibrillation. Initial observations using 4D-flow MRI indicate that left atrial peak velocity and vorticity are reproducible and temporally stable flow biomarkers, which appear robust against variations in heart rate, blood pressure, and rhythm [95]. However, further investigations are warranted.

Third, the prognostic significance of alterations in intracardiac flow dynamics in patients with HF remains largely undefined, as does their additional value in relation to other parameters derived from cardiac imaging techniques. Similarly, although initial observations, particularly involving HDFs, have been published, it is still uncertain whether the analysis of LV flow dynamics can inform or assist in the pharmacological treatment of HF patients.

Fourth, it is important to note that current clinical investigations on intracardiac flow dynamics in HF patients often involve a limited number of participants, and the follow-up duration is typically insufficient to draw reliable conclusions. Multicenter studies with larger sample sizes and extended follow-up periods are essential to confirm initial observations.

Finally, the assessment of flow dynamics within the LV has generally been performed using parameters or indices related to the entire LV, especially when utilizing KE or KEL. However, it is now possible to evaluate regional blood flow KE at different levels and in various segments of the same heart cavity [96]. Applying this analysis to HF patients could potentially enhance our understanding of cardiac dysfunction.

Conclusions

Current evidence based on advanced cardiac imaging techniques, including echo-PIV, VFM, HyperDoppler, strain-based analysis of HDFs, and 4D-flow MRI, indicates that in patients with HF the blood flow patterns in the LV cavity are significantly altered. These alterations can be visually described and quantified through various parameters that characterize vortex geometry, strength, and intensity, as well as VFT, KE, KEL/KED, KEF, and HDFs.

Currently available data highlight the significant potential of intracardiac flow dynamics analysis to identify cardiac dysfunction, particularly at an early stage. However, studies are still insufficient to guide the treatment of HF and to stratify prognosis based on vortex flow dynamics. These represent important challenges for future research.

Abbreviations

4D	Four-dimensional
BSI	Blood speckle imaging
CCT	Cardiac computed tomography
CDV	Color Doppler velocimetry
CFD	Computational fluid dynamics
CRT	Cardiac resynchronization therapy
DCM	Dilated cardiomyopathy
DF	Direct flow
EDV	End-diastolic volume
ESV	End-systolic volume
HDF	Hemodynamic force
HF	Heart failure
HFmrEF	Heart failure mildly reduced ejection fraction
HFpEF	Heart failure preserved ejection fraction
HFrEF	Heart failure reduced ejection fraction
KE	Kinetic energy
KEL	Kinetic energy loss
KED	Kinetic energy dissipation
KEF	Kinetic energy fluctuation
ICM	Ischemic cardiomyopathy
IRF	Isovolumic relaxation flow
IVCT	Isovolumetric contraction time
IVPG	Intraventricular pressure gradient
IVRT	Isovolumetric relaxation time
LBBB	Left bundle branch block
LV	Left ventricle
LVAD	Left ventricular assist device
LV-EF	Left ventricular ejection fraction
LVOT	Left ventricular outflow tract
MACE	Major adverse cardiac event
MI	Myocardial infarction
MR	Mitral regurgitation
MRI	Magnetic resonance imaging
NYHA	New York Heart Association
PIV	Particle image velocimetry
SV	Stroke volume
VFM	Vector flow mapping
VFT	Vortex formation time

Acknowledgements
Not applicable.

Author contributions
DM wrote the main manuscript text. LS prepared the figures. RB prepared the tables. AC, GP, LS, RB, SN reviewed the manuscript.

Funding
The authors declare that no funding was received for the preparation of this manuscript.

Data availability
No datasets were generated or analysed during the current study.

Declarations

Ethics approval and consent to participate
Not applicable.

Consent for publication
Not applicable.

Competing interests
The authors declare no competing interests.

Received: 18 February 2025 / Accepted: 31 March 2025
Published online: 19 May 2025

References

1. McDonagh TA, Metra M, Adamo M, Gardner RS, Baumbach A, Böhm M, et al. 2021 ESC guidelines for the diagnosis and treatment of acute and chronic heart failure. Eur Heart J. 2021;42:3599–726. https://doi.org/10.1093/eurheartj/ehab368.
2. Mele D, Andrade A, Bettencourt P, Moura B, Pestelli G, Ferrari R. From left ventricular ejection fraction to cardiac hemodynamics: role of echocardiography in evaluating patients with heart failure. Heart Fail Rev. 2020;25:217–30. https://doi.org/10.1007/s10741-019-09826-w.
3. Mele D, Smarrazzo V, Pedrizzetti G, Capasso F, Pepe M, Severino S, et al. Intracardiac flow analysis: techniques and potential clinical applications. J Am Soc Echocardiogr. 2019;32:319–32. https://doi.org/10.1016/j.echo.2018.10.018.
4. Serio L, Beccari R, Nistri S, Cecchetto A, Pedrizzetti G, Mele D. Intracardiac flow dynamics in mitral regurgitation: state of the Art. Eur Heart J - Imaging Methods Pract. 2025;qyaf022. https://doi.org/10.1093/ehjimp/qyaf022.
5. Fiorencis A, Pepe M, Smarrazzo V, Martini M, Severino S, Pergola V, et al. Non-invasive evaluation of intraventricular flow dynamics by the hyperdoppler technique: first application to normal subjects, athletes, and patients with heart failure. J Clin Med. 2022;11:2216. https://doi.org/10.3390/jcm11082216.
6. Lantz J, Gupta V, Henriksson L, Karlsson M, Persson A, Carlhäll C-J, et al. Intracardiac flow at 4D CT: comparison with 4D flow MRI. Radiology. 2018;289:51–8. https://doi.org/10.1148/radiol.2018173017.
7. Bennati L, Puppini G, Giambruno V, Luciani GB, Vergara C. Image-Based computational fluid dynamics to compare two repair techniques for mitral valve prolapse. Ann Biomed Eng. 2024;52:3295–311. https://doi.org/10.1007/s10439-024-03597-8.
8. Collia D, Vukicevic M, Meschini V, Zovatto L, Pedrizzetti G. Simplified mitral valve modeling for prospective clinical application of left ventricular fluid dynamics. J Comput Phys. 2019;398:108895. https://doi.org/10.1016/j.jcp.2019.108895.
9. Mele D, Smarrazzo V, Pedrizzetti G, Bertini M, Ferrari R. Intracardiac flow analysis in cardiac resynchronization therapy: A new challenge? Echocardiography. 2019;36:1919–29. https://doi.org/10.1111/echo.14477.
10. Ngiam JN, Liong TS, Pramotedham T, Sia C-H, Jou E, Kong WK-F, et al. Left ventricular vortex formation time: emerging clinical applications and limitations. Singap Med J. 2023. https://doi.org/10.4103/singaporemedj.SMJ-2022-132.
11. Mele D, Beccari R, Pedrizzetti G. Effect of aging on intraventricular kinetic energy and energy dissipation. J Cardiovasc Dev Dis. 2023;10:308. https://doi.org/10.3390/jcdd10070308.
12. Aimo A, Panichella G, Fabiani I, Garofalo M, Fanizzi AI, Ragagnin M, et al. Assessing cardiac mechanics through left ventricular haemodynamic forces. Eur Heart J Imaging Methods Pract. 2024;2:qyae077. https://doi.org/10.1093/ehjimp/qyae077.
13. Vallelonga F, Airale L, Tonti G, Argulian E, Milan A, Narula J, et al. Introduction to hemodynamic forces analysis: moving into the new frontier of cardiac deformation analysis. J Am Heart Assoc. 2021;10:e023417. https://doi.org/10.1161/JAHA.121.023417.

14. Bermejo J, Benito Y, Alhama M, Yotti R, Martínez-Legazpi P, Del Villar CP, et al. Intraventricular vortex properties in nonischemic dilated cardiomyopathy. Am J Physiol Heart Circ Physiol. 2014;306:H718–29. https://doi.org/10.1152/ajpheart.00697.2013.
15. Mutluer FO, Van Der Velde N, Voorneveld J, Bosch JG, Roos-Hesselink JW, Van Der Geest RJ, et al. Evaluation of intraventricular flow by multimodality imaging: a review and meta-analysis. Cardiovasc Ultrasound. 2021;19:38. https://doi.org/10.1186/s12947-021-00269-8.
16. Bolger A, Heiberg E, Karlsson M, Wigström L, Engvall J, Sigfridsson A, et al. Transit of blood flow through the human left ventricle mapped by cardiovascular magnetic resonance. J Cardiovasc Magn Reson. 2007;9:741–7. https://doi.org/10.1080/10976640701544530.
17. Eriksson J, Dyverfeldt P, Engvall J, Bolger AF, Ebbers T, Carlhäll CJ. Quantification of presystolic blood flow organization and energetics in the human left ventricle. Am J Physiol Heart Circ Physiol. 2011;300:H2135–41. https://doi.org/10.1152/ajpheart.00993.2010.
18. Mangual JO, Kraigher-Krainer E, De Luca A, Toncelli L, Shah A, Solomon S, et al. Comparative numerical study on left ventricular fluid dynamics after dilated cardiomyopathy. J Biomech. 2013;46:1611–7. https://doi.org/10.1016/j.jbiomech.2013.04.012.
19. Postigo A, Viola F, Chazo C, Martínez-Legazpi P, González-Mansilla A, Rodríguez-González E, et al. Assessment of blood flow transport in the left ventricle using ultrasound. Validation against 4-D flow cardiac magnetic resonance. Ultrasound Med Biol. 2022;48:1822–32. https://doi.org/10.1016/j.ultrasmedbio.2022.05.007.
20. Agati L, Cimino S, Tonti G, Cicogna F, Petronilli V, De Luca L, et al. Quantitative analysis of intraventricular blood flow dynamics by echocardiographic particle image velocimetry in patients with acute myocardial infarction at different stages of left ventricular dysfunction. Eur Heart J Cardiovasc Imaging. 2014;15:1203–12. https://doi.org/10.1093/ehjci/jeu106.
21. Pedrizzetti G, La Canna G, Alfieri O, Tonti G. The vortex—an early predictor of cardiovascular outcome? Nat Rev Cardiol. 2014;11:545–53. https://doi.org/10.1038/nrcardio.2014.75.
22. Pasipoularides A. Mechanotransduction mechanisms for intraventricular diastolic vortex forces and myocardial deformations: part 1. J Cardiovasc Transl Res. 2015;8:76–87. https://doi.org/10.1007/s12265-015-9611-y.
23. Brancaccio M, Hirsch E, Notte A, Selvetella G, Lembo G, Tarone G. Integrin signalling: the tug-of-war in heart hypertrophy. Cardiovasc Res. 2006;70:422–33. https://doi.org/10.1016/j.cardiores.2005.12.015.
24. Pasipoularides A. Mechanotransduction mechanisms for intraventricular diastolic vortex forces and myocardial deformations: part 2. J Cardiovasc Transl Res. 2015;8:293–318. https://doi.org/10.1007/s12265-015-9630-8.
25. Kuwahara K, Wang Y, McAnally J, Richardson JA, Bassel-Duby R, Hill JA, et al. TRPC6 fulfills a calcineurin signaling circuit during pathologic cardiac remodeling. J Clin Invest. 2006;116:3114–26. https://doi.org/10.1172/JCI27702.
26. Jiang F, Yin K, Wu K, Zhang M, Wang S, Cheng H, et al. The mechanosensitive Piezo1 channel mediates heart mechano-chemo transduction. Nat Commun. 2021;12:869. https://doi.org/10.1038/s41467-021-21178-4.
27. Linke W. Sense and stretchability: the role of Titin and Titin-associated proteins in myocardial stress-sensing and mechanical dysfunction. Cardiovasc Res. 2007;S0008636307001551. https://doi.org/10.1016/j.cardiores.2007.03.029.
28. Lindsey SE. Mechanical regulation of cardiac development. Front Physiol. 2014;5. https://doi.org/10.3389/fphys.2014.00318.
29. Hove JR, Köster RW, Forouhar AS, Acevedo-Bolton G, Fraser SE, Gharib M. Intracardiac fluid forces are an essential epigenetic factor for embryonic cardiogenesis. Nature. 2003;421:172–7. https://doi.org/10.1038/nature01282.
30. Dirkx E, Da Costa Martins PA, De Windt LJ. Regulation of fetal gene expression in heart failure. Biochim Biophys Acta Mol Basis Dis. 2013;1832:2414–24. https://doi.org/10.1016/j.bbadis.2013.07.023.
31. Hong G-R, Pedrizzetti G, Tonti G, Li P, Wei Z, Kim JK, et al. Characterization and quantification of vortex flow in the human left ventricle by contrast echocardiography using vector particle image velocimetry. JACC Cardiovasc Imaging. 2008;1:705–17. https://doi.org/10.1016/j.jcmg.2008.06.008.
32. Zhang H, Liu L, Chen L, Ma N, Zhou L, Liu Y, et al. The evolution of intraventricular vortex during ejection studied by using vector flow mapping. Echocardiography. 2013;30:27–36. https://doi.org/10.1111/j.1540-8175.2012.01806.x.
33. Chan BT, Yeoh HK, Liew YM, Dokos S, Al Abed A, Chee KH, et al. Quantitative analysis of intraventricular flow-energetics and vortex in ischaemic hearts. Coron Artery Dis. 2018;29:316–24. https://doi.org/10.1097/MCA.0000000000000596.
34. Fukuda N, Itatani K, Kimura K, Ebihara A, Negishi K, Uno K, et al. Prolonged vortex formation during the ejection period in the left ventricle with low ejection fraction: a study by vector flow mapping. J Med Ultrason. 2014;41:301–10. https://doi.org/10.1007/s10396-014-0530-3.
35. Kim I-C, Hong G-R, Pedrizzetti G, Shim CY, Kang S-M, Chung N. Usefulness of left ventricular vortex flow analysis for predicting clinical outcomes in patients with chronic heart failure: A quantitative vorticity imaging study using contrast echocardiography. Ultrasound Med Biol. 2018;44:1951–9. https://doi.org/10.1016/j.ultrasmedbio.2018.05.015.
36. Cimino S, Pedrizzetti G, Tonti G, Canali E, Petronilli V, De Luca L, et al. In vivo analysis of intraventricular fluid dynamics in healthy hearts. Eur J Mech B Fluids. 2012;35:40–6. https://doi.org/10.1016/j.euromechflu.2012.03.014.
37. Tang C, Zhu Y, Zhang J, Niu C, Liu D, Liao Y, et al. Analysis of left ventricular fluid dynamics in dilated cardiomyopathy by echocardiographic particle image velocimetry. Echocardiography. 2018;35:56–63. https://doi.org/10.1111/echo.13732.
38. Chan JSK, Lau DHH, Fan Y, Lee AP-W. Fragmented vortex in heart failure with reduced ejection fraction: A prospective vector flow mapping study. Ultrasound Med Biol. 2023;49:982–8. https://doi.org/10.1016/j.ultrasmedbio.2022.12.001.
39. Gharib M, Rambod E, Kheradvar A, Sahn DJ, Dabiri JO. Optimal vortex formation as an index of cardiac health. Proc Natl Acad Sci USA. 2006;103:6305–8. https://doi.org/10.1073/pnas.0600520103.
40. Poh KK, Lee LC, Shen L, Chong E, Tan YL, Chai P, et al. Left ventricular fluid dynamics in heart failure: echocardiographic measurement and utilities of vortex formation time. Eur Heart J Cardiovasc Imaging. 2012;13:385–93. https://doi.org/10.1093/ejechocard/jer288.
41. Eriksson J, Bolger AF, Ebbers T, Carlhäll C-J. Four-dimensional blood flow-specific markers of LV dysfunction in dilated cardiomyopathy. Eur Heart J Cardiovasc Imaging. 2013;14:417–24. https://doi.org/10.1093/ehjci/jes159.
42. Kanski M, Arvidsson PM, Töger J, Borgquist R, Heiberg E, Carlsson M, et al. Left ventricular fluid kinetic energy time curves in heart failure from cardiovascular magnetic resonance 4D flow data. J Cardiovasc Magn Reson. 2015;17:111. https://doi.org/10.1186/s12968-015-0211-4.
43. Svalbring E, Fredriksson A, Eriksson J, Dyverfeldt P, Ebbers T, Bolger AF, et al. Altered diastolic flow patterns and kinetic energy in subtle left ventricular remodeling and dysfunction detected by 4D flow MRI. PLoS ONE. 2016;11:e0161391. https://doi.org/10.1371/journal.pone.0161391.
44. Riva A, Saitta S, Sturla F, Disabato G, Tondi L, Camporeale A, et al. Left ventricle diastolic vortex ring characterization in ischemic cardiomyopathy: insight into atrio-ventricular interplay. Med Biol Eng Comput. 2024;62:3671–85. https://doi.org/10.1007/s11517-024-03154-4.
45. Carlhäll CJ, Bolger A. Passing strange: flow in the failing ventricle. Circ Heart Fail. 2010;3:326–31. https://doi.org/10.1161/CIRCHEARTFAILURE.109.911867.
46. Pedrizzetti G, Numata R, Collia D, Pedrizzetti G, Zovatto L, Banerjee A. A scenario for heart failure during the filling phase. Sci Rep. 2024;14:22760. https://doi.org/10.1038/s41598-024-74155-4.
47. Li C, Bai W, Liu Y, Tang H, Rao L. Dissipative energy loss within the left ventricle detected by vector flow mapping in diabetic patients with controlled and uncontrolled blood glucose levels. Int J Cardiovasc Imaging. 2017;33:1151–8. https://doi.org/10.1007/s10554-017-1100-8.
48. Wang Y, Ma R, Ding G, Hou D, Li Z, Yin L, et al. Left ventricular energy loss assessed by vector flow mapping in patients with prediabetes and type 2 diabetes mellitus. Ultrasound Med Biol. 2016;42:1730–40. https://doi.org/10.1016/j.ultrasmedbio.2016.03.008.
49. Chen X, Wang Y, Wang W, Yuan L, Qi Z, Song D. Assessment of left ventricular energy loss using vector flow mapping in patients with stages 1–3 chronic kidney disease. BMC Cardiovasc Disord. 2020;20:355. https://doi.org/10.1186/s12872-020-01640-9.
50. Zhong Y, Liu Y, Wu T, Song H, Chen Z, Zhu W, et al. Assessment of left ventricular dissipative energy loss by vector flow mapping in patients with End-Stage renal disease. J Ultrasound Med. 2016;35:965–73. https://doi.org/10.7863/ultra.15.06009.
51. Wang W, Wang Y, Chen X, Yuan L, Bai H. Evaluation of left ventricular diastolic function based on flow energetic parameters in chronic kidney disease with diastolic dysfunction. Echocardiography. 2019;36:567–76. https://doi.org/10.1111/echo.14264.
52. Amaki M, Nakabo A, Abe H, Pedrizzetti G, Narula J, Sengupta P. Left ventricular vortex formation and altered flow energetics in diastolic dysfunction. J Am Coll Cardiol. 2014;63:A992. https://doi.org/10.1016/S0735-1097(14)60992-X.
53. Han Y, Huang L, Li Z, Ma N, Li Q, Li Y, et al. Relationship between left ventricular isovolumic relaxation flow patterns and mitral inflow patterns studied by

using vector flow mapping. Sci Rep. 2019;9:16264. https://doi.org/10.1038/s41598-019-52680-x.
54. Berlot B, Moya Mur JL, Jug B, Rodríguez Muñoz D, Megias A, Casas Rojo E, et al. Effect of diastolic dysfunction on intraventricular velocity behavior in early diastole by flow mapping. Int J Cardiovasc Imaging. 2019;35:1627–36. https://doi.org/10.1007/s10554-019-01612-x.
55. Kheradvar A, Assadi R, Falahatpisheh A, Sengupta PP. Assessment of transmitral vortex formation in patients with diastolic dysfunction. J Am Soc Echocardiogr. 2012;25:220–7. https://doi.org/10.1016/j.echo.2011.10.003.
56. Eriksson J, Zajac J, Alehagen U, Bolger AF, Ebbers T, Carlhäll C-J. Left ventricular hemodynamic forces as a marker of mechanical dyssynchrony in heart failure patients with left bundle branch block. Sci Rep. 2017;7:2971. https://doi.org/10.1038/s41598-017-03089-x.
57. Arvidsson PM, Töger J, Pedrizzetti G, Heiberg E, Borgquist R, Carlsson M, et al. Hemodynamic forces using four-dimensional flow MRI: an independent biomarker of cardiac function in heart failure with left ventricular dyssynchrony? Am J Physiol Heart Circ Physiol. 2018;315:H1627–39. https://doi.org/10.1152/ajpheart.00112.2018.
58. Zajac J, Eriksson J, Alehagen U, Ebbers T, Bolger AF, Carlhäll C-J. Mechanical dyssynchrony alters left ventricular flow energetics in failing hearts with LBBB: a 4D flow CMR pilot study. Int J Cardiovasc Imaging. 2018;34:587–96. https://doi.org/10.1007/s10554-017-1261-5.
59. Töger J, Kanski M, Arvidsson PM, Carlsson M, Kovács SJ, Borgquist R, et al. Vortex-ring mixing as a measure of diastolic function of the human heart: Phantom validation and initial observations in healthy volunteers and patients with heart failure. Magn Reson Imaging. 2016;43:1386–97. https://doi.org/10.1002/jmri.25111.
60. Ashkir Z, Myerson S, Neubauer S, Carlhäll C-J, Ebbers T, Raman B. Four-dimensional flow cardiac magnetic resonance assessment of left ventricular diastolic function. Front Cardiovasc Med. 2022;9:866131. https://doi.org/10.3389/fcvm.2022.866131.
61. Pedrizzetti G, Arvidsson PM, Töger J, Borgquist R, Domenichini F, Arheden H, et al. On estimating intraventricular hemodynamic forces from endocardial dynamics: A comparative study with 4D flow MRI. J Biomech. 2017;60:203–10. https://doi.org/10.1016/j.jbiomech.2017.06.046.
62. Lapinskas T, Pedrizzetti G, Stoiber L, Düngen H-D, Edelmann F, Pieske B, et al. The intraventricular hemodynamic forces estimated using routine CMR cine images. JACC Cardiovasc Imaging. 2019;12:377–9. https://doi.org/10.1016/j.jcmg.2018.08.012.
63. Arvidsson PM, Nelsson A, Magnusson M, Smith JG, Carlsson M, Arheden H. Hemodynamic force analysis is not ready for clinical trials on HFpEF. Sci Rep. 2022;12:4017. https://doi.org/10.1038/s41598-022-08023-4.
64. Backhaus SJ, Uzun H, Rösel SF, Schulz A, Lange T, Crawley RJ, et al. Hemodynamic force assessment by cardiovascular magnetic resonance in HFpEF: A case-control substudy from the HFpEF stress trial. eBioMedicine. 2022;86:104334. https://doi.org/10.1016/j.ebiom.2022.104334.
65. Airale L, Vallelonga F, Forni T, Leone D, Magnino C, Avenatti E, et al. A novel approach to left ventricular filling pressure assessment: the role of hemodynamic forces analysis. Front Cardiovasc Med. 2021;8:704909. https://doi.org/10.3389/fcvm.2021.704909.
66. Son J-W, Park W-J, Choi J-H, Houle H, Vannan MA, Hong G-R, et al. Abnormal left ventricular vortex flow patterns in association with left ventricular apical thrombus formation in patients with anterior myocardial Infarction: – A quantitative analysis by contrast Echocardiography–. Circ J. 2012;76:2640–6. https://doi.org/10.1253/circj.CJ-12-0360.
67. Cordero CD, Rossini L, Martinez-Legazpi P, Del Villar CP, Benito Y, Barrio A, et al. Prediction of intraventricular thrombosis by quantitative imaging of stasis: A pilot Color-Doppler study in patients with acute myocardial infarction. J Am Coll Cardiol. 2015;65:A1310. https://doi.org/10.1016/S0735-1097(15)61310-9.
68. Garg P, Van Der Geest RJ, Swoboda PP, Crandon S, Fent GJ, Foley JRJ, et al. Left ventricular thrombus formation in myocardial infarction is associated with altered left ventricular blood flow energetics. Eur Heart J Cardiovasc Imaging. 2019;20:108–17. https://doi.org/10.1093/ehjci/jey121.
69. Demirkiran A, Hassell MECJ, Garg P, Elbaz MSM, Delewi R, Greenwood JP, et al. Left ventricular four-dimensional blood flow distribution, energetics, and vorticity in chronic myocardial infarction patients with/without left ventricular thrombus. Eur J Radiol. 2022;150:110233. https://doi.org/10.1016/j.ejrad.2022.110233.
70. Sakakibara T, Suwa K, Ushio T, Wakayama T, Alley M, Saotome M, et al. Intra-Left ventricular hemodynamics assessed with 4D flow magnetic resonance imaging in patients with left ventricular thrombus. Int Heart J. 2021;62:1287–96. https://doi.org/10.1536/ihj.20-792.
71. Rossini L, Braun OÖ, Brambatti M, Benito Y, Mizeracki A, Miramontes M, et al. Intraventricular flow patterns in patients treated with left ventricular assist devices. ASAIO J. 2021;67:74–83. https://doi.org/10.1097/MAT.0000000000001158.
72. Nabeta T, Itatani K, Miyaji K, Ako J. Vortex flow energy loss reflects therapeutic effect in dilated cardiomyopathy. Eur Heart J. 2015;36:637–637. https://doi.org/10.1093/eurheartj/ehu394.
73. Monosilio S, Filomena D, Luongo F, Sannino M, Cimino S, Neccia M, et al. Cardiac and vascular remodeling after 6 months of therapy with Sacubitril/Valsartan: mechanistic insights from advanced echocardiographic analysis. Front Cardiovasc Med. 2022;9:883769. https://doi.org/10.3389/fcvm.2022.883769.
74. Fabiani I, Pugliese NR, Pedrizzetti G, Tonti G, Castiglione V, Chubuchny V, et al. Haemodynamic forces predicting remodelling and outcome in patients with heart failure treated with Sacubitril/valsartan. ESC Heart Fail. 2023;10:2927–38. https://doi.org/10.1002/ehf2.14346.
75. Mele D, Trevisan F, Fiorencis A, Smarrazzo V, Bertini M, Ferrari R. Current role of echocardiography in cardiac resynchronization therapy: from cardiac mechanics to flow dynamics analysis. Curr Heart Fail Rep. 2020;17:384–96. https://doi.org/10.1007/s11897-020-00484-w.
76. Goliasch G, Goscinska-Bis K, Caracciolo G, Nakabo A, Smolka G, Pedrizzetti G, et al. CRT improves LV filling dynamics. JACC Cardiovasc Imaging. 2013;6:704–13. https://doi.org/10.1016/j.jcmg.2013.04.004.
77. Pedrizzetti G, Martiniello AR, Bianchi V, D'Onofrio A, Caso P, Tonti G. Cardiac fluid dynamics anticipates heart adaptation. J Biomech. 2015;48:388–91. https://doi.org/10.1016/j.jbiomech.2014.11.049.
78. Pedrizzetti G, Martiniello AR, Bianchi V, D'Onofrio A, Caso P, Tonti G. Changes in electrical activation modify the orientation of left ventricular flow momentum: novel observations using echocardiographic particle image velocimetry. Eur Heart J Cardiovasc Imaging. 2016;17:203–9. https://doi.org/10.1093/ehjci/jev137.
79. Cimino S, Palombizio D, Cicogna F, Cantisani D, Reali M, Filomena D, et al. Significant increase of flow kinetic energy in nonresponders patients to cardiac resynchronization therapy. Echocardiography. 2017;34:709–15. https://doi.org/10.1111/echo.13518.
80. Dal Ferro M, De Paris V, Collia D, Stolfo D, Caiffa T, Barbati G, et al. Left ventricular response to cardiac resynchronization therapy: insights from hemodynamic forces computed by speckle tracking. Front Cardiovasc Med. 2019;6:59. https://doi.org/10.3389/fcvm.2019.00059.
81. Laenens D, Van Der Bijl P, Galloo X, Rossi AC, Tonti G, Reiber JH, et al. Evolution of Echocardiography-Derived hemodynamic force parameters after cardiac resynchronization therapy. Am J Cardiol. 2023;209:138–45. https://doi.org/10.1016/j.amjcard.2023.09.098.
82. Laenens D, Van Der Bijl P, Galloo X, Rossi AC, Tonti G, Reiber JHC, et al. Association between echocardiography-derived haemodynamic force parameters and left ventricular reverse remodelling after cardiac resynchronization therapy. Eur Heart J Cardiovasc Imaging. 2024;25:1721–33. https://doi.org/10.1093/ehjci/jeae181.
83. Pola K, Roijer A, Borgquist R, Ostenfeld E, Carlsson M, Bakos Z, et al. Hemodynamic forces from 4D flow magnetic resonance imaging predict left ventricular remodeling following cardiac resynchronization therapy. J Cardiovasc Magn Reson. 2023;25:45. https://doi.org/10.1186/s12968-023-00955-8.
84. Siciliano M, Migliore F, Badano L, Bertaglia E, Pedrizzetti G, Cavedon S, et al. Cardiac resynchronization therapy by multipoint pacing improves response of left ventricular mechanics and fluid dynamics: a three-dimensional and particle image velocimetry echo study. Europace. 2017;19:1833–40. https://doi.org/10.1093/europace/euw331.
85. Rodríguez Muñoz D, Moya Mur JL, Moreno J, Fernández-Golfín C, Franco E, Berlot B, et al. Mitral-Aortic flow reversal in cardiac resynchronization therapy: coupling with ejection and impact of variations in atrioventricular delay. Circ Arrhythm Electrophysiol. 2017;10. https://doi.org/10.1161/CIRCEP.116.004927.
86. Rodríguez Muñoz D, Moya Mur JL, Moreno J, Fernández-Golfín C, Franco E, Monteagudo JM, et al. Energy dissipation in resynchronization therapy: impact of atrioventricular delay. J Am Soc Echocardiogr. 2019;32:744–e7541. https://doi.org/10.1016/j.echo.2019.01.018.
87. Rossini L, Martinez-Legazpi P, Vu V, Fernández-Friera L, Del Pérez C, Rodríguez-López S, et al. A clinical method for mapping and quantifying blood stasis in the left ventricle. J Biomech. 2016;49:2152–61. https://doi.org/10.1016/j.jbiomech.2015.11.049.
88. Aigner P, Schweiger M, Fraser K, Choi Y, Lemme F, Cesarovic N, et al. Ventricular flow field visualization during mechanical circulatory support in the

assisted isolated beating heart. Ann Biomed Eng. 2020;48:794–804. https://doi.org/10.1007/s10439-019-02406-x.
89. May-Newman K, Wong YK, Adamson R, Hoagland P, Vu V, Dembitsky W. Thromboembolism is linked to intraventricular flow stasis in a patient supported with a left ventricle assist device. ASAIO J. 2013;59:452–5. https://doi.org/10.1097/MAT.0b013e318299fced.
90. Vu V, Rossini L, Del Alamo JC, Dembitsky W, Gray RA, May-Newman K. Benchtop models of Patient-Specific intraventricular flow during heart failure and LVAD support. J Biomech Eng. 2023;145:111010. https://doi.org/10.1115/1.4063147.
91. Schinkel AFL, Akin S, Strachinaru M, Muslem R, Bowen D, Yalcin YC, et al. Evaluation of patients with a heartmate 3 left ventricular assist device using echocardiographic particle image velocimetry. J Ultrasound. 2021;24:499–503. https://doi.org/10.1007/s40477-020-00533-z.
92. Abe H, Caracciolo G, Kheradvar A, Pedrizzetti G, Khandheria BK, Narula J, et al. Contrast echocardiography for assessing left ventricular vortex strength in heart failure: a prospective cohort study. Eur Heart J Cardiovasc Imaging. 2013;14:1049–60. https://doi.org/10.1093/ehjci/jet049.
93. Stoll VM, Hess AT, Rodgers CT, Bissell MM, Dyverfeldt P, Ebbers T, et al. Left ventricular flow analysis: novel imaging biomarkers and predictors of exercise capacity in heart failure. Circ Cardiovasc Imaging. 2019;12:e008130. https://doi.org/10.1161/CIRCIMAGING.118.008130.
94. Vos JL, Raafs AG, Henkens MTHM, Pedrizzetti G, Van Deursen CJ, Rodwell L, et al. CMR-derived left ventricular intraventricular pressure gradients identify different patterns associated with prognosis in dilated cardiomyopathy. Eur Heart J Cardiovasc Imaging. 2023;24:1231–40. https://doi.org/10.1093/ehjci/jead083.
95. Spartera M, Pessoa-Amorim G, Stracquadanio A, Von Ende A, Fletcher A, Manley P, et al. Left atrial 4D flow cardiovascular magnetic resonance: a reproducibility study in sinus rhythm and atrial fibrillation. J Cardiovasc Magn Reson. 2021;23:29. https://doi.org/10.1186/s12968-021-00729-0.
96. Niu X, Dun Y, Li G, Zhang H, Zhang B, Pan Z, et al. Evaluation of left ventricular blood flow kinetic energy in patients with acute myocardial infarction by 4D flow MRI: a preliminary study. BMC Med Imaging. 2024;24:131. https://doi.org/10.1186/s12880-024-01310-8.

Publisher's note

Springer Nature remains neutral with regard to jurisdictional claims in published maps and institutional affiliations.